AD-A116 292 PENNSYLVANIA STATE UNIV UNIVERSITY PARK APPLIED RESE--ETC F/G 14/2
HYDRODYNAMIC TEST FACILITIES AT ARL/PSU.(U)
FEB 82 R E HENDERSON, B R PARKIN N00024-79-C-6043
UNCLASSIFIED ARL/PSU/TM-82-66 NL

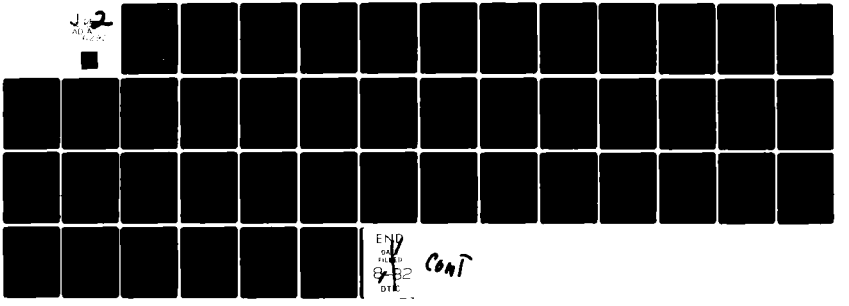

CONT


A
29

(6)

HYDRODYNAMIC TEST FACILITIES AT ARL/PSU

R. E. Henderson and B. R. Parkin

Technical Memorandum
File No. 82-66
12 February 1982
Contract No. N00024-79-C-6043

Copy No. 49

The Pennsylvania State University
APPLIED RESEARCH LABORATORY
Post Office Box 30
State College, PA 16801

Approved for Public Release
Distribution Unlimited

NAVY DEPARTMENT

NAVAL SEA SYSTEMS COMMAND

SECURITY CLASSIFICATION OF THIS PAGE (When Data Entered)

REPORT DOCUMENTATION PAGE		READ INSTRUCTIONS BEFORE COMPLETING FORM
1. REPORT NUMBER TM 82-66	2. GOVT ACCESSION NO. AD-A116 292	3. RECIPIENT'S CATALOG NUMBER
4. TITLE (and Subtitle) HYDRODYNAMIC TEST FACILITIES AT ARL/PSU		5. TYPE OF REPORT & PERIOD COVERED Technical Memorandum
		6. PERFORMING ORG. REPORT NUMBER
7. AUTHOR(s) R. E. Henderson and B. R. Parkin		8. CONTRACT OR GRANT NUMBER(s) N00024-79-C-6043
9. PERFORMING ORGANIZATION NAME AND ADDRESS Applied Research Laboratory Post Office Box 30 State College, PA 16801		10. PROGRAM ELEMENT, PROJECT, TASK AREA & WORK UNIT NUMBERS
11. CONTROLLING OFFICE NAME AND ADDRESS Naval Sea Systems Command Department of the Navy Washington, DC 20362		12. REPORT DATE 12 February 1982 13. NUMBER OF PAGES 40
14. MONITORING AGENCY NAME & ADDRESS(if different from Controlling Office)		15. SECURITY CLASS. (of this report) UNCLASSIFIED 15a. DECLASSIFICATION/DOWNGRADING SCHEDULE

16. DISTRIBUTION STATEMENT (of this Report)

Approved for public release. Distribution unlimited
Per NAVSEA - March 2, 1982.

17. DISTRIBUTION STATEMENT (of the abstract entered in Block 20, if different from Report)

18. SUPPLEMENTARY NOTES

19. KEY WORDS (Continue on reverse side if necessary and identify by block number)

hydrodynamics, test, facilities, water tunnels

20. ABSTRACT (Continue on reverse side if necessary and identify by block number)

A discussion is presented of the major advances in hydrodynamic testing which have been demonstrated in the Fluids Engineering Department during the past 15 years.

DD FORM 1 JAN 73 1473 EDITION OF 1 NOV 65 IS OBSOLETE

SECURITY CLASSIFICATION OF THIS PAGE (When Data Entered)

Subject: Hydrodynamic Test Facilities at ARL/PSU

References: See page 15.

Abstract: A discussion is presented of the major advances in hydrodynamic testing which have been demonstrated in the Fluids Engineering Department during the past 15 years.

Acknowledgments: The research reported here was sponsored by the Naval Sea Systems Command. The authors would like to express their appreciation to all of the members of the staff of the Fluids Engineering Department for their contributions in providing these advanced test capabilities. The results presented here are drawn from the work of many individuals, so many in fact, that it is not possible to cite them all by name.

Table of Contents

1.0 INTRODUCTION

The design and operational characteristics of the 1.22 m diameter, high speed water tunnel (the Garfield Thomas Water Tunnel) operated by the Fluids Engineering Department of the Applied Research Laboratory, the Pennsylvania State University (ARL/PSU) have been documented in a number of reports and papers written during its first 18 years of operation [1-3]. Since the last of these papers was written in 1967, the capabilities of the Garfield Thomas Water Tunnel (GTWT) to address hydrodynamic problems have been significantly extended. These new capabilities include: (1) the measurement of cavitation noise and noise in the absence of cavitation; (2) the measurement of the dynamic forces generated on model propulsors operating on a model vehicle; (3) the reduction of the turbulence level in its test section to 0.1% with an integral scale of 1.25 cm, by the addition of honeycomb in the settling section; and (4) the development of electro-optical measuring techniques. In addition to these new capabilities, efforts have continued in the area of tunnel/model interference and its influence on model drag. By the use of tunnel wall flow correcting liners, it is possible to predict accurately the propulsion characteristics of large powered models.

The purpose of this paper is to discuss these developments in the hydrodynamic experimental capabilities of the GTWT during the past 15 years. Also to be discussed are a number of complimentary test facilities, both water and air tunnels, which contribute to the solution of hydrodynamic problems. These discussions will be accompanied by examples of test results which demonstrate the successful employment of these test facilities.

2.0 DESCRIPTION OF FACILITIES

In the following discussion of the hydrodynamic experimental capabilities at ARL/PSU, results obtained from experiments conducted in five of its major test facilities will be presented. These facilities include:

(1) the Garfield Thomas Water Tunnel (GTWT) with its 1.22 m x 4.27 m cylindrical test section and a maximum test section velocity of 18.29 m/s;

(2) the "small" water tunnel which has both a 0.305 m x 0.762 m cylindrical and a 0.508 m x 0.114 m x 0.762 m rectangular test section with a maximum test section velocity of 24.38 m/s;

(3) the 0.152 m diameter water tunnel with a maximum velocity of 27.4 m/s which can be used as a closed circuit pump loop;

(4) the ultra-high speed water tunnel with a 38.1 mm diameter test section and a maximum velocity of 83.8 m/s; and

(5) the axial flow research fan which is an open-circuit subsonic air tunnel used to study the steady and dynamic flow through propulsor blade rows.

A complete description of the operating characteristics of each of these facilities, together with a circuit schematic, can be found in Appendix A.

3.0 VEHICLE POWERING TESTS

The standard facility used to determine the powering or propulsion characteristics of a marine vehicle is the towing tank, and is essential for the determination of wave drag. They are also useful for cases in which free-surface effects are not important, such as completely submerged vehicles. However, towing tank tests to determine the propulsion characteristics of a completely submerged vehicle will usually have a limiting test velocity of the order of 5-8 m/s due to the effects of surface waves and water-piercing strut interference drag. The resulting Reynolds number is then often too low to allow accurate scaling of the powering data to the prototype vehicle.

Surface interference effects can be eliminated for completely submerged vehicles by conducting the powering tests in a water tunnel. In a large water tunnel the tests can usually be conducted at higher test velocities, 10-12.2 m/s in the GTWT, and hence at higher Reynolds numbers than in a towing tank with the same model. The attainment of higher Reynolds numbers minimizes the possible errors in scaling the powering data. At the same time, the water tunnel allows propulsor cavitation characteristics to be determined with the propulsor operated in the vehicle boundary layer. While these points are obvious advantages in the testing of completely submerged vehicles, the additional factors of tunnel wall interference and horizontal buoyancy must be considered.

In the late 1950's a study was conducted at ARL/PSU on the use of tunnel wall flow correcting liners to minimize these drag interference effects [4], [5]. The usefulness of this technique depends upon the accurate calculation of the flow field over the model when operated both with and without the tunnel walls present. The tunnel walls are then altered for each model by inserting a tunnel wall liner which is designed to give, except for fluid-frictional effects, the same flow over the model as it is predicted to experience without the tunnel walls present, i.e., a "free-field" condition, Figure 1.

The use of tunnel wall liners has proven to be a very successful means to provide the same boundary layer velocity profile at the aft-end of a model as measured in a towing tank or in a very large wind tunnel where model/wall interference is negligible. In the case of models whose total length is greater than the test section length, 4 m, a section of the model's parallel mid-section must be removed.

This removed section is simulated by the addition of a screen, or screens, on the remaining vehicle surface. The length of screen is selected so as to add the same frictional resistance as the removed parallel midsection. This provides the same boundary layer velocity profile as with the complete model. Figure 2 shows the agreement of the circumferential mean velocity profile measured on a shortened 0.61 m maximum diameter model in the 1.22 m diameter test section with data measured with a total length model in a towing tank.

Experience has shown that while the liners provide a correct velocity distribution, they cannot be designed, manufactured and installed with sufficient accuracy to eliminate completely the effects of horizontal buoyancy on vehicle drag [5]. During the past 10 years a study of this problem has shown that it is possible to correct empirically for these inaccuracies. Experience and the theory of interference for an axially symmetric body in a circular test section [1] indicate that if the ratio of the model diameter (d) to the test section diameter (D) is less than 1/9, the interference drag will be within the accuracy of the drag measurements. It is therefore possible to measure the drag on a scaled model whose $d < D/9$, calculate the residual or pressure drag coefficient of the model by subtracting the calculated friction drag coefficient from the measured total drag, assume that the residual drag coefficient does not change with Reynolds number, and calculate the total drag coefficient of a model whose $d > D/9$ as a function of Reynolds number. Since this calculation does not include the effects of tunnel wall interference, it represents a baseline or reference for tests with the large model. These same reference data can also be obtained from tests of the large model in a towing tank.

Once the variation of model drag coefficient with Reynolds number is known, these data can be used to "calibrate" the tunnel/model installation and determine the wall interference and horizontal buoyancy associated with the large model, Figure 3. This represents a correction which must be applied to the net axial force, thrust-drag, on a model with an operating propeller. The use of a tunnel wall liner then assures that the propeller operates in the correct boundary layer profile and it minimizes the magnitude of the wall interference correction. Recent tests using liners constructed of fiberglass segments and a model of $d = 0.53D$, showed this correction to be approximately 8 percent of the total model drag.

Figure 4 shows a example of the application of this procedure to the prediction of the powering performance of a particular vehicle. This figure compares the velocity of a completely submerged vehicle and its propeller torque as predicted from water tunnel tests with values measured during free-running field trials.

4.0 CAVITATION TESTS

At the ARL/PSU, cavitation tests are conducted in the 1.22 m, 0.305 m, 0.147 m, and 3.81 cm water tunnels. In the 1.22 m GTWT most of the cavitation studies are concerned with cavitation inception, cavitation noise and cavitation scaling experiments on large scale bodies, hydrofoils and propellers. The 0.305 m tunnel is used to conduct fundamental studies of cavitation scaling, vortex cavitation, cavitation noise, and both ventilated and supercavitating flows with small scale stationary bodies and hydrofoils. The influence of polymers on cavitation inception and scaling have been studied in the 0.147 m tunnel, together with cavity flows on hydrofoils. The small, ultra-high speed 3.81 cm tunnel was originally built by NASA to study thermodynamic effects on cavitation in a liquid operating near its critical point. In addition, the NASA tunnel has been used to study the effect of velocity on cavitation damage since it can attain a maximum velocity of 83.8 m/s.

Generally, the kinds of measurements needed for cavitation research are the same as those required for the study of non-cavitating flows. This is so because it is first necessary to understand the non-cavitating flow and to then relate its characteristics to the conditions under which cavitation occurs. However, certain experimental techniques have become particularly useful in cavitation research and these techniques will be emphasized here.

4.1 Nuclei Measurements

An important research topic these days is the determination of the way cavitation nuclei influence the occurrence of cavitation. Although present knowledge on this subject is incomplete, a number of investigators around the world are studying various aspects of this problem using various methods of measurement. At ARL/PSU both light-scattering and holographic techniques have been used with the emphasis on the measurement of free-stream nuclei size distributions. For example, it was found in a joint research program with the California Institute of Technology (CIT) [6] that light scattering and holographic measurements produced significantly different nuclei size distributions when measurements were made by both methods in the same facility. Such dual measurements were made at CIT in their High Speed and Low Turbulence tunnels [7], [8], and supplementary light-scattering measurements were made in the ARL/PSU 0.305 m tunnel. In these experiments the light-scattering unit was of a type similar to that proposed by Keller [9]. The single detector/counter used is illustrated in Figure 5 and the calibration curves shown in Figure 6 compare the results obtained at CIT and ARL/PSU. Comparative nuclei distributions measured by the light scattering and holographic techniques in the CIT High Speed Water Tunnel are shown in Figure 7. A schematic of the holographic apparatus is shown in Figure 8. It

was concluded from these experiments that the light scattering technique was not able to discriminate between solid particles and air bubbles in the flow.

As a result of these findings, recent studies at ARL/PSU have concentrated on the development of a dual-detector technique which, with the use of Mie-scattering theory, can give information about the shape of the particle. This permits the light scattering technique to discriminate between microbubbles and particulates, Figure 9. The results to date indicate that this modified Keller system offers the potential of screening particulates from the microbubble counts [10]. The main task remaining before this approach can be called successful is to conduct a detail error analysis in order to resolve the system inaccuracy introduced by the data reduction algorithm. Because the light scattering technique offers the chance of getting nearly real-time nuclei distribution data while a cavitation test is in progress, this improvement of the Keller system is worth pursuing.

Assuming that valid nuclei size distributions can be obtained while a cavitation experiment is underway, the question of how such distributions influence the development of cavitation on a body must be studied. Such a study can be conducted if the cavitation events can be related to such flow features as the boundary layer thickness or whether or not the flow is separated. Schlieren flow visualization is an effective way to show the relationship of cavitation inception and its type to the state of the boundary layer [11]. Measurements of this type have been performed in the ARL/PSU 0.305 m tunnel using light scattering and schlieren systems simultaneously as illustrated in Figure 10 [12].

Of course holographic photography can be used for flow visualization with excellent results in both cavitating and non-cavitating flows.

4.2 Cavitation Damage

In the introductory remarks of this section it was noted that one use of the NASA tunnel and its very high velocity, has been to study the process of cavitation damage [13]. Recent studies at ARL/PSU have confirmed the sixth-power of the free-stream velocity scaling relation reported by previous investigators. In these studies it was possible to obtain nearly a four-fold increase in velocity, from about 15 m/s to 60 m/s. A fact not previously reported is that the pitting rate in the incubation zone is sensitive to, and inversely proportional to, the dissolved air content. Therefore it was possible to correct all of the data to a standard air content of 8.9 ppm so that data for all investigations over a 10,000 to 1 range in damage rates could be brought into remarkable agreement, Figure 11. It is important to stress that this investi-

gation involved the study of pitting on a body with the occurrence of weight loss. With this restriction it was found that damage in the form of individual pits had a one-to-one correspondence with the cavitation bubble collapse energy, and the change in this energy with free-stream velocity could be inferred.

5.0 ACOUSTIC TESTS

The GTWT was designed to provide the capability to conduct research on torpedo propellers operated in a specified vehicle/control fin wake [1]. With the wake flow produced by the installation of the actual vehicle or a scaled model, the measurement of the forces on the vehicle and its propeller and the occurrence of cavitation on the propeller were the primary performance characteristics studied. While the inception of cavitation was detected acoustically, as well as visually, the GTWT was not used to conduct detailed acoustic tests during its first 20 years of operation. Fortunately, the design of the GTWT was directed towards quiet and vibration free operation. The success in achieving these goals has permitted the development of a capability to conduct tests of both cavitating and non-cavitating propeller noise.

5.1 Cavitation Noise

The GTWT was designed so that one side of its test section could be fitted with an acoustic tank in which a traversing reflector hydrophone could be mounted, Figure 12. With the hydrophone focused on the centerline of the test section, it measures the noise radiated from a model located opposite the 27 cm x 60 cm plexiglass windows.

The receiver is a Celesco LC-10 hydrophone located at the focus of the ellipsoidal reflector. This hydrophone is calibrated by placing an omni-directional sound projector with a known response in the test section and driving it over a frequency range of 1-120 kHz. The calibration is conducted with the sound projector located on the test section centerline and at a constant distance off-centerline in each of four or more circumferential positions, Figure 13. This latter approach permits an average sensitivity to be determined diminishes the influence of spurious acoustic modes that are observed when the projector is on the centerline. It is also more representative of the noise radiated by a propeller since cavitation will normally appear first near the tip of the blades.

The influence of the test section on the directivity of the reflector hydrophone is shown by Figure 14. In this figure the directivity measured at 20 kHz in the test section is compared with the same measurement conducted in the free field [14]. It is obvious that this arrangement is acceptable if the hydrophone is positioned in the center of the window, but is restricted by the metal webs between the windows. To overcome this restriction an

acoustically transparent hatch cover has been procurred for the GTWT. This special hatch replaces the original metal access cover to the test section with a large (0.4 m x 3.0 m) continuous plexiglass window. A tank is located over this large window which is filled with water and allows the installation of additional hydrophones. This permits an unobstructed acoustical scanning of the model in the test section. This new hatch also provides improved viewing of cavitation.

Figure 12 shows the installation of a stationary hydrofoil in the test section for the purpose of determining the effects of Reynolds number on cavitation noise. Using this test setup a series of four geometrically similar, but differently sized, hydrofoils were tested. The variation of the noise associated with leading edge sheet cavitation with Reynolds number was determined when the cavitation cavity was 1/3 of the hydrofoil chord length, Figure 15. This figure demonstrates the effect of laminar boundary layer separation on cavitation and its noise. In separate flow visualization tests, the 3.81 and 7.62 cm chord hydrofoils were shown to be experiencing a long and a short laminar separation bubble, respectively. On the other hand, the 15.24 and 30.48 cm hydrofoils experienced a non-separated turbulent boundary layer. The complete results of this study can be found in Reference [15].

The cavitation noise radiated by a propeller can also be determined from these test setups. The propeller can either be mounted in an inclined position to duplicate the wake from the drive shaft and struts, Figure 16, or with a model hull attached to a flat plate which spans the test section, Figure 17. In both cases the influence of the free surface and Froude scaling is ignored. Using either of these installations it is possible to determine the variation of propeller cavitation noise as a function of Reynolds number. With these data it is possible to develop model-to-prototype cavitation noise scaling laws if full-scale data are available.

5.2 Non-Cavitating Noise

In addition to cavitation noise, the GTWT can be used to study non-cavitating propeller noise. This is accomplished with an array of 69 parallel-wired hydrophones located in a hydrodynamic fairing at the end of the tunnel diffuser in front of the first set of turning vanes, Figure 18. This sensor permits the far-field radiated noise to be measured at frequencies > 300 Hz. When used in conjunction with other sensors located in the test section, dual-channel signal processing can be used to identify sources of propeller noise and paths of propogation.

The measurement of non-cavitating model propeller noise requires the model motor and drive system to operate with a minimum level of

mechanical noise in order to assure a sufficient propeller signal-to-noise ratio. This is accomplished with a specially designed quiet motor/dynamometer. The background noise spectrum is measured with the quieted model motor/dynamometer operating with a tunnel velocity and a rotating bare hub. When a model propeller is installed on the model and operated at the same tunnel velocity and RPM, its measured noncavitating noise is above the background noise by the amount shown in Figure 19.

To study the mechanisms by which propellers and turbomachines generate radiated noise, an air-breathing anechoic chamber is available for operation with the Axial Flow Research Fan (AFRF). This chamber has internal dimensions of 2.7 x 3.2 m and is anechoic at frequencies above 230 Hz. It is equipped with polyurethane foam wedges and provides a flow of air to the AFRF through its top and bottom edges. The chamber can also operate as a stand-alone anechoic chamber by removal of the AFRF.

Employing this arrangement and instrumentation to measure the dynamic forces and pressures on the AFRF blades (these are described in a later section), one can determine the acoustic transfer function by conducting simultaneous measurements of the radiated noise. It is also possible to determine the effects of blade geometry on radiated noise since the AFRF is designed to accommodate systematic changes in blade number, blade pitch angle and blade lift coefficient.

In all of the arrangements described above, the recording and analysis of the acoustic signals are accomplished by a number of real-time signal processors. The processed data can be transmitted to a high-speed digital computer. Here the data are corrected for hydrophone sensitivity and system gains and plotted in a format consistent with the type of signal analysis performed. A block diagram of this data reduction system is shown in Figure 20.

6.0 DYNAMIC FORCE TESTS

A major concern in the field of hydrodynamics is the generation of dynamic forces on the propeller and hull of a marine vehicle since this can result in excessive structural vibration. The ability to control this vibration requires the capability to measure the hydrodynamic forces which cause the vibration. At ARL/PSU dynamic propeller forces are measured either as the dynamic shaft thrust or as the dynamic lift and moment on a section of the propeller.

On the other hand the measurement of the low frequency, essentially quasi-steady, dynamic forces on a vehicle which is made to move in a prescribed motion, can be used to determine the closed-loop control and maneuvering characteristics of the vehicle. These dynamic

forces are measured using a Planar Motion Mechanism which is operated in the GTWT. These dynamic forces are then used to determine the hydrodynamic stability derivatives on models of completely submerged vehicles.

6.1 Dynamic Propeller Forces

The measurement of the total dynamic response of a propeller at ARL/PSU is limited to the measurement of the dynamic shaft thrust alone. While the dynamic thrust is only one component of the entire dynamic response of the propeller, it is a major component in most cases. Further, the combination of accurate dynamic shaft thrust measurements and an analytical method to predict all of the components of the propeller dynamic shaft response permits the remaining components to be inferred.

The propeller dynamic shaft thrust dynamometer used at ARL/PSU is shown in Figure 21. The sensor is a peizoelectric crystal which reacts to the dynamic thrust through a hardened steel hemispherical ball on the propeller hub. The dynamometer is designed to be compliant only in the thrust direction and is located within the propeller drive shaft. While the compliancy will limit the response of the dynamometer at higher frequencies, experience has shown that it is possible to obtain a flat sensor response to frequencies in the order of 700 Hz. This is usually sufficient to permit the measurement of the first- and second-harmonics of the dynamic thrust.

This dynamometer has been used to study the dynamic shaft thrust generated on a propeller operated in spatially non-uniform inflows and in various temporally varying, turbulent, inflows. Some typical results from these studies are shown in Figure 22, where the measured dynamic thrust on a free-stream propeller operated in a homogeneous turbulent inflow is shown. These measured values are compared with predictions from a method by Thompson [16]. This method also predicts all of the components of the dynamic force and moment on the propeller shaft due to operation in a spatially non-uniform inflow.

To determine the mechanisms which cause the dynamic shaft response of a propeller, it is necessary to study the dynamic response of the individual blades. To accomplish this, a strain gage dynamometer has been developed which measures the dynamic lift and moment on a section of a rotating blade, Figure 23.

To date this concept has been used with a rotor operated in the AFRF. A series of tests has been conducted in spatially non-uniform inflows to determine the effects of blade pitch angle (β), solidity or expanded area ratio, and reduced frequency on the dynamic lift and moment [17]. Such data provide the opportunity to assess the various analytical methods which are available to predict the dynamic

lift and moment on a rotating blade. These data also provide insight into what blade geometries will minimize the level of the blade's dynamic response to a known non-uniform inflow.

While this individual blade dynamometer is limited in its frequency response to < 160 Hz, it is possible to test at reduced frequencies, based on the chord length, of nearly 10. The definition of reduced frequency used here is:

$$2\pi \text{ (chord length) } \cos(\beta)/(\text{distortion wavelength})$$

These values of reduced frequency are experienced in practice and are obtained by using large blade chord lengths, 15.24 cm, and varying the wavelength of the distorted inflow between 7.9 and 118 cm.

6.2 Planar Motion Mechanism

The prediction of the trajectory and dynamic motion of a marine vehicle requires a knowledge of how the forces on the vehicle change with time and vehicle attitude. This knowledge can be obtained by forcing a model of the vehicle into a known time-dependent motion and measuring the resulting forces. This permits the vehicle's stability derivatives to be determined and used in the equations of motion.

An accepted means to obtain the stability derivatives is to conduct tests with a Planar Motion Mechanism (PMM). The GTWT has been equipped with a PMM which is fitted to a special tunnel hatch cover and permits the evaluation of small (d < 20 cm) axisymmetric models, Figure 24. This system can drive the model in a pure heaving motion as shown in Figure 24, a pure pitching motion by having the actuators in phase, or in a combined motion. The maximum frequency of oscillation is 10 Hz.

The unique feature of the GTWT PMM is that it can be used to determine the effects of cavitation the vehicle's response and both quasi-steady and dynamic hydrodynamic forces can be studied.

7.0 FLOW FIELD MEASUREMENTS

It is well recognized that an extremely important part of hydrodynamic testing is the ability to measure the velocity and pressure fields associated with a particular test setup. As a result, the development of pressure probes, hot-film and hot-wire probes, and more recently laser Doppler velocimeters is a common undertaking in a hydrodynamic test laboratory. While flow field measurements have been a routine capability at ARL/PSU for many years, there have been some recent developments which extend these capabilities. These include: (1) the use of nylon mono-filament mini-tufts for

surface flow visualization; (2) the development of miniature 5-hole probes with a total diameter of 1.67 mm; and (3) the measurement of the flow field relative to a rotating propeller. Each of these recent developments is described below.

7.1 Mini-Tuft Flow Visualization

The visualization of surface flows and flow separation with small wool-tufts is a common practice in wind tunnel testing. The adaptation of this method to water tunnels is difficult, however, because of the wetting of the tufts. In both air and water the size of the tufts can produce an interference with the surface flow and result in a false conclusion. Following a development in the aerospace field, ARL/PSU has demonstrated the use of nylon mono-filament mini-tufts with a diameter of 0.03 mm in water [18].

These mini-tufts are attached to the surface with an epoxy cement at the positions where the surface flows are of interest. They are typically 12 mm in length and, as such, are barely visible to the naked eye. To overcome this limitation the mono-filament is coated with a fluorescent dye which makes them appear to be many times their actual size when viewed in an ultravoilet light. This provides a very effective means to visualize flow separation without the problem of the markers interfering with the flow field.

While the use of these mini-tufts has been satisfactorily demonstrated in the ARL/PSU 0.305 m diameter water tunnel, they are still not operational in the 1.22 m GTWT. This restriction is due to the inability to transmit enough ultraviolet light through the GTWT windows and nearly 0.6 m of water to satisfactorily illuminated the mini-tufts. This can probably be overcome by using a stronger light source and windows which absorb less of the ultraviolet light.

7.2 Miniature 5-Hole Probes

Five-hole pressure probes are common in all hydrodynamic laboratories [19]. One of the restrictions of commercially available 5-hole probes is their size and the subsequent interference effect which they have on the flow, particularly shear flows such as the wake behind a fin. As a result, many laboratories attempt to manufacture their own 5-hole probes to provide smaller overall dimensions. At ARL/PSU such a development has lead to the use of a 5-hole probe whose maximum diameter d = 1.67 mm.

The usefulness of this probe is shown in Figure 25 where the vector sum of the radial and tangential components of the velocity downstream of a set of stationary fins is plotted. This representation clearly shows the tip vortices and detailed wake structure associated with each fin. The ability of these small probes to

measure this kind of detail provides a more exact Fourier representation of the flow field, which is important in the analysis of the dynamic response of a propeller.

7.3 Flow Relative to a Rotating Propeller

The hydrodynamic propeller designer is always concerned with the flow field relative to the blades of a rotating propeller. In the past this information has been lacking since it is extremely difficult to obtain. However, the development of the laser doppler velocimeter provides a technique which makes these measurements possible.

The data acquisition system employed at ARL/PSU to measure the velocities relative to a rotating propeller is shown in Figure 26. The heart of this system is the data control system which was designed and built at ARL/PSU. This system receives a signal from an encoder attached to the rotating shaft, takes this signal and chooses the correct instant when the laser beam is to be focused at a pre-selected position relative to the rotating propeller, accepts the scattered light at that instant and passes on to the next point. By changing the specified position it is possible to obtain a survey of the velocity field relative to the propeller. Figure 27 is an example of such a survey.

The AFRF is a specialized airflow facility for the study of axial-flow turbomachinery rotor and stator. It also has the capability to conduct flow surveys relative to the rotating blades, but using conventional probes. The rotor hub is large enough to house a special mechanism which rotates with the rotor and will position a probe within the channel between the blades. This mechanism is described in Reference [20].

8.0 SUMMARY

This report has presented a brief discussion of the major improvements that have occurred in the test capabilities of the ARL/PSU hydrodynamic test facilities during the past ten years. These advances include the development of (1) corrections for tunnel wall interference on powered model drag measurements, (2) electro-optic techniques for measuring cavitation nuclei distributions and velocity fields, (3) techniques to study cavitation damage using high velocity flows, (4) the capability to measure cavitating and non-cavitating propeller noise, (5) dynamometers to measure propeller and model dynamic forces, and (6) improved methods to measure and visualize hydrodynamic flow fields.

9.0 REFERENCES

[1] Ross, D., J. M. Robertson and R. B. Power, "Hydrodynamic Design of the 48-inch Water Tunnel at the Pennsylvania State University," SNAME TRANSACTIONS, Vol. 56, pp. 5-29, 1948.

[2] Lehman, A. F., "The Garfield Thomas Water Tunnel," Ordnance Research Laboratory Report NORD 16597-56, September 1959.

[3] Lehman, A. F. and T. E. Peirce, "The Garfield Thomas Water Tunnel," UNDERWATER MISSILE PROPULSION, Ed L. Greiner, Compass Publications, Inc., Arlington, VA, pp. 401-420, 1967.

[4] Lehman, A. F., J. H. Light and T. E. Peirce, "Elimination of Water-Tunnel Interaction With a Coaxial Test Body by a Flow-Correcting Liner," Ordnance Research Laboratory Report NORD 16597-39, July 1958.

[5] Peirce, T. E., "Tunnel Wall Interference Effects on Drag and Pitching Moment of an Axisymmetric Body," Ph.D. Thesis, Pennsylvania State University, December 1964.

[6] Billet, M. L. and E. M. Gates, "A Comparison of Two Optical Techniques for Measuring Cavitation Nuclei," TRANSACTIONS OF ASME, JOURNAL OF FLUIDS ENGINEERING, Vol. 103, pp. 8-13, 1981.

[7] Ward, T. M., "The Hydrodynamics Laboratory at the California Institute of Technology," TRANSACTIONS OF ASME, JOURNAL OF FLUIDS ENGINEERING, Vol. 98, pp. 740-748, 1976.

[8] Gates, E. M., "The Influence of Free-Stream Turbulence, Free-Stream Nuclei Populations and Drag Reducing Polymers on Cavitation Inception," California Institute of Technology, Division of Engineering and Applied Science, Report No. 183-2, 1977.

[9] Keller, A. P., "The Influence of the Cavitation Nucleus on Cavitation Inception, Investigated With the Light Scattering Method," TRANSACTIONS OF ASME, JOURNAL OF BASIC ENGINEERING, Vol. 94, pp. 917-925, 1972.

[10] Billet, M. L. and C. B. Yungkurth, "Light Scattering System: Analysis and Calibration," ASME Symposium on Measurements in Polyphase Flows, St. Louis, MO, June 1982.

[11] Arakeri, V. H. and A. J. Acosta, "Cavitation Inception Observations on Axisymmetric Bodies at Supercritical Reynolds Numbers," JOURNAL FOR SHIP RESEARCH, Vol. 20, No. 1, pp. 40-50, 1976.

[12] Gates, E. M., M. L. Billet, J. Katz, K. K. Ooi, J. W. Holl, A. J. Acosta, "Cavitation and Nuclei Distributions - Joint ARL/CIT Experiments," California Institute of Technology, Division of Engineering and Applied Science, Report No. E 244.1, September 1979.

[13] Stinebring, D. R., J. W. Holl and R. E. A. Arndt, "Two Aspects of Cavitation Damage in the Incubation Zone: Scaling by Energy Considerations and Leading Edge Damage," TRANSACTIONS OF ASME, JOURNAL OF FLUIDS ENGINEERING, Vol. 102, pp. 481-485, 1980.

[14] Lauchle, G. C., "Acoustic Characteristics of the ARL/FEU Ellipsoidal Reflecting Hydrophone," Applied Research Laboratory TM 76-15, February 1976.

[15] Billet, M. L. and D. E. Thompson, "Blade Surface Cavitation Noise," PROCEEDINGS OF ASCE, IAHR/AIHR and ASME JOINT SYMPOSIUM ON FLUID MACHINERY, Vol. II, Fort Collins, CO, June 1978.

[16] Thompson, D. E., "Propeller Time-Dependent Forces Due to Non Uniform Inflow," Ph.D. Thesis, Pennsylvania State University, 1976.

[17] Bruce, E. P., "Axial Flow Rotor Unsteady Performance," Ph.D. Thesis, Pennsylvania State University, 1979.

[18] Stinebring, D. R. and A. L. Treaster, "The Use of Fluorescent Mini-Tufts for Hydrodynamic Flow Field Visualization," Applied Research Laboratory TM 80-07, January 1980.

[19] Treaster, A. L. and A. M. Yocum, "The Calibration and Application of Five-Hole Probes," Instrument Society of America Transactions, Vol. 18, No. 3, pp. 23-34, 1979.

[20] Pierzga, M. J., "Experimental Verification of the Streamline Curvature Numerical Analysis Method Applied to the Flow Through an Axial Flow Fan," M.S. Thesis, Pennsylvania State University, 1980.

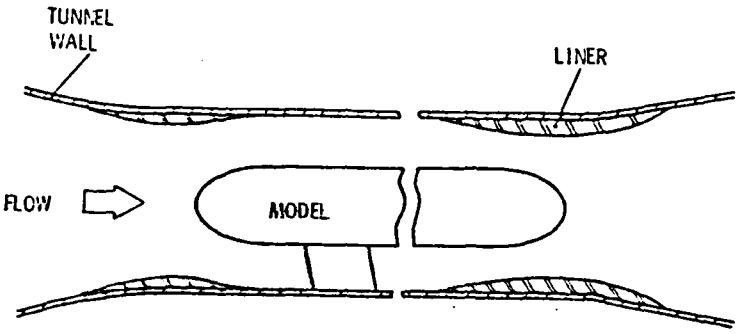

Figure 1. Installation of Model With Tunnel Wall Liner in GTWT

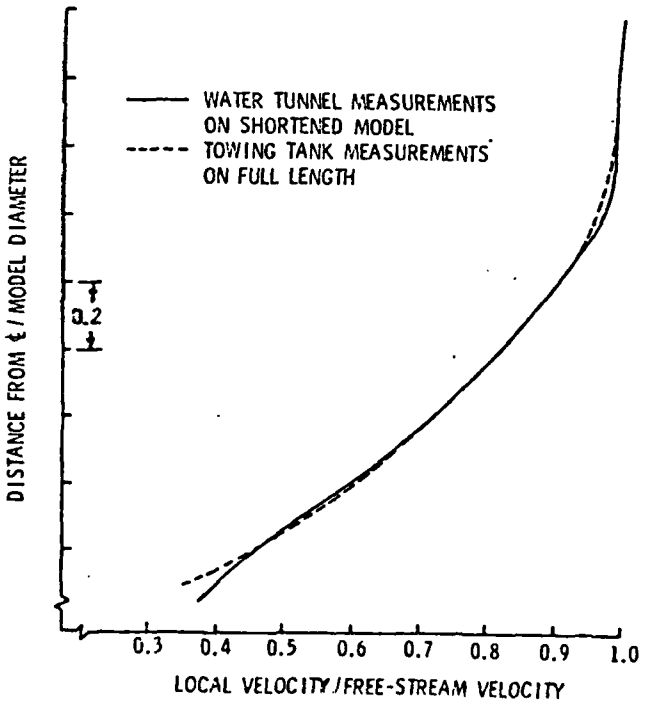

Figure 2. Comparison of 0.61 m Diameter Model Velocity Profile Measured in Water Tunnel and Towing Tank

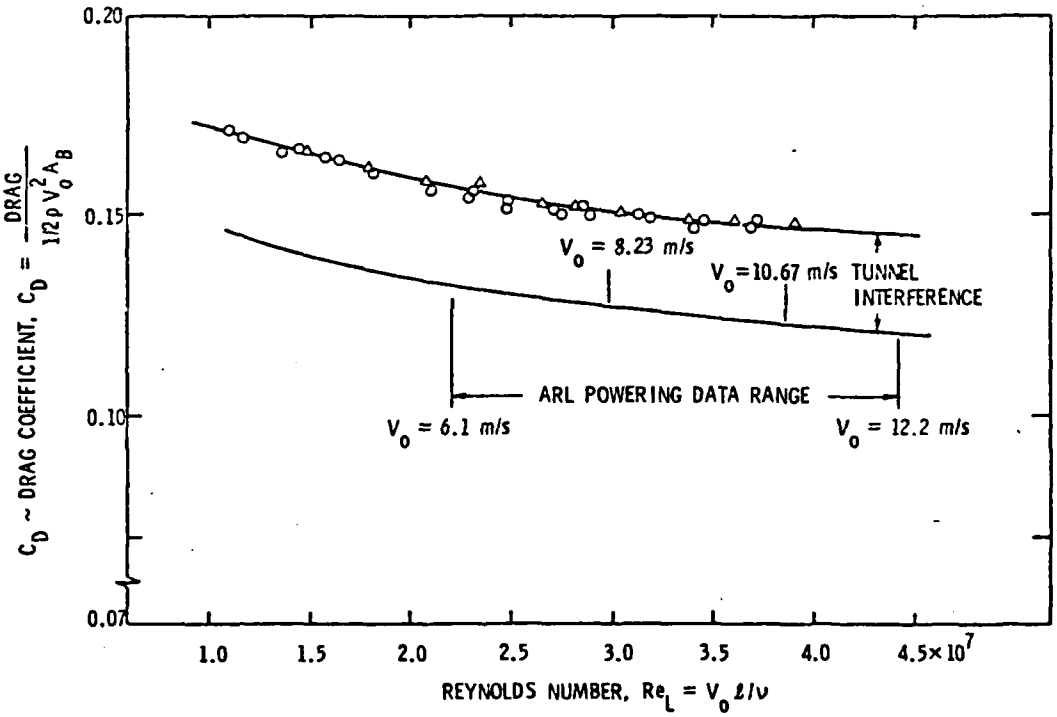

Figure 3. C_D vs Reynolds; Determination of Wall Interference

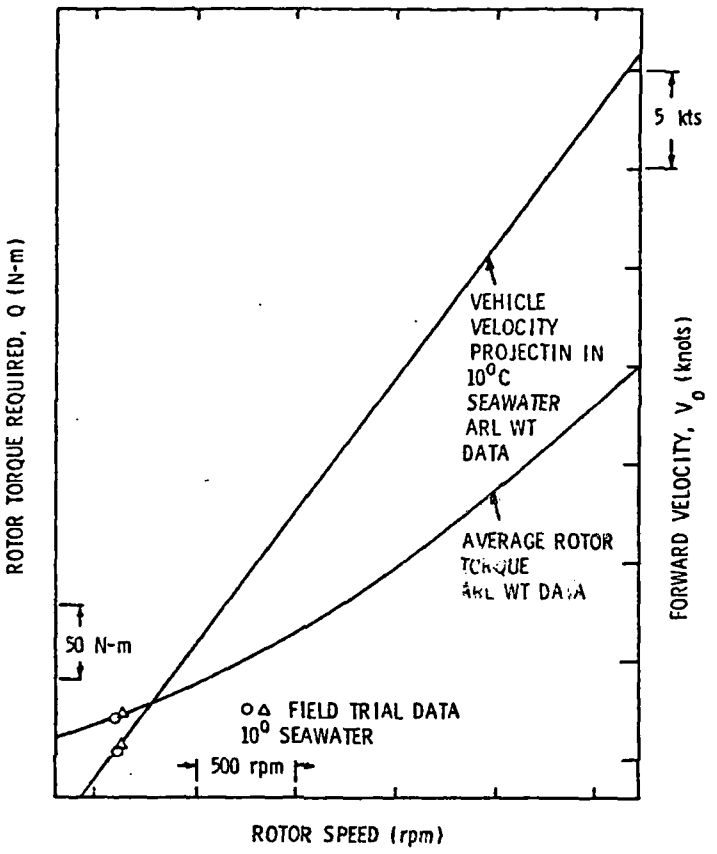

Figure 4. Comparison of Water Tunnel and Free-Field Propulsion Data

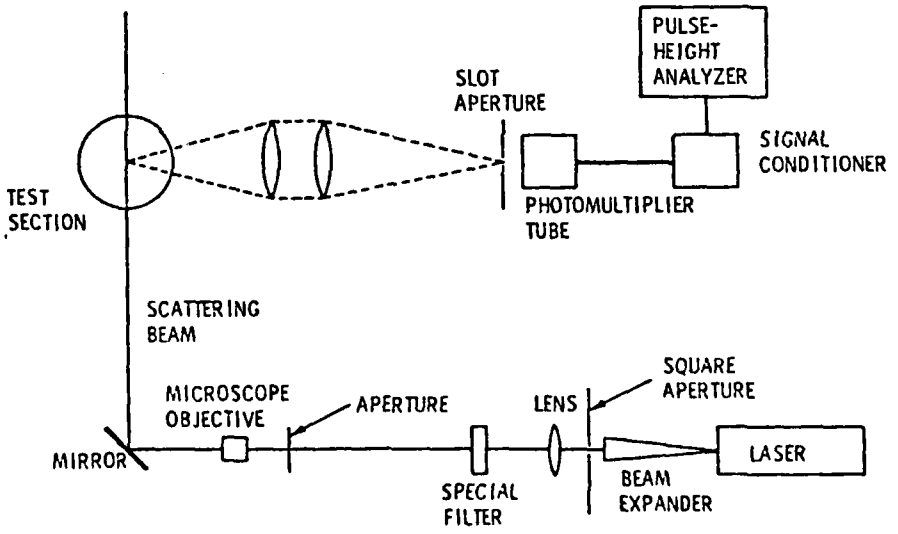

Figure 5. Schematic of the Light Scattering Nuclei Counter

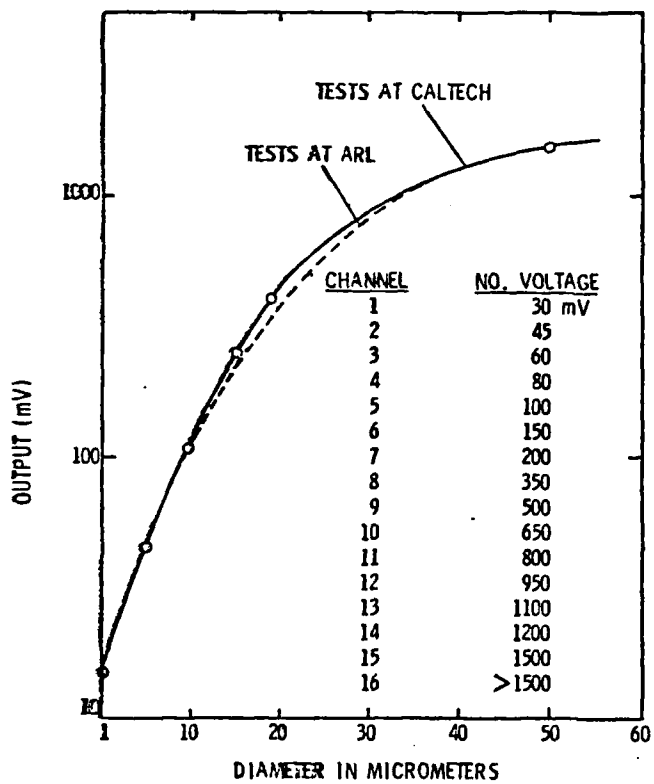

Figure 6. Calibration of Light Scattering Nuclei Counter at CIT and ARL/PSU

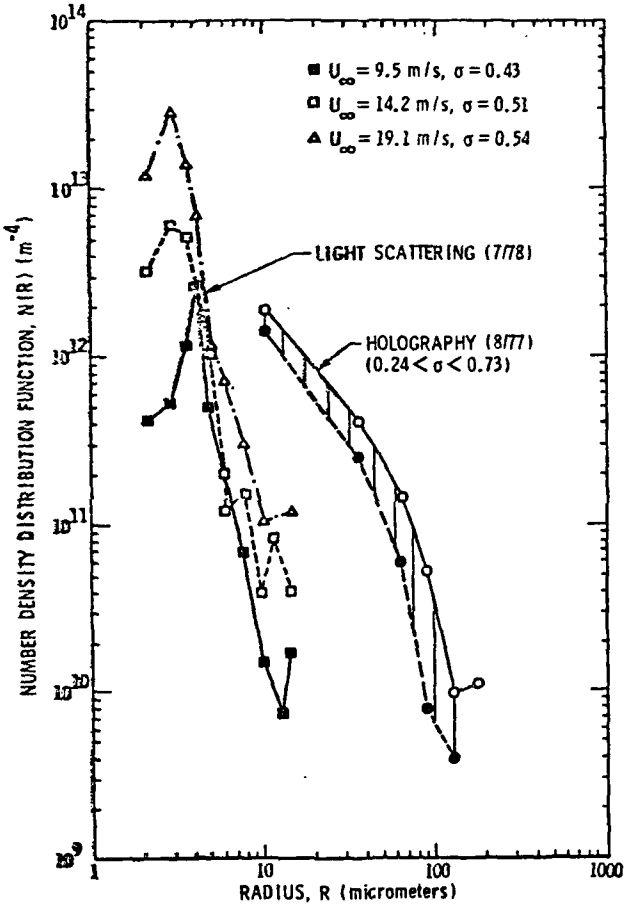

Figure 7. A Comparison of Nuclei Distributions Measured in Light Scattering and Holographic Systems

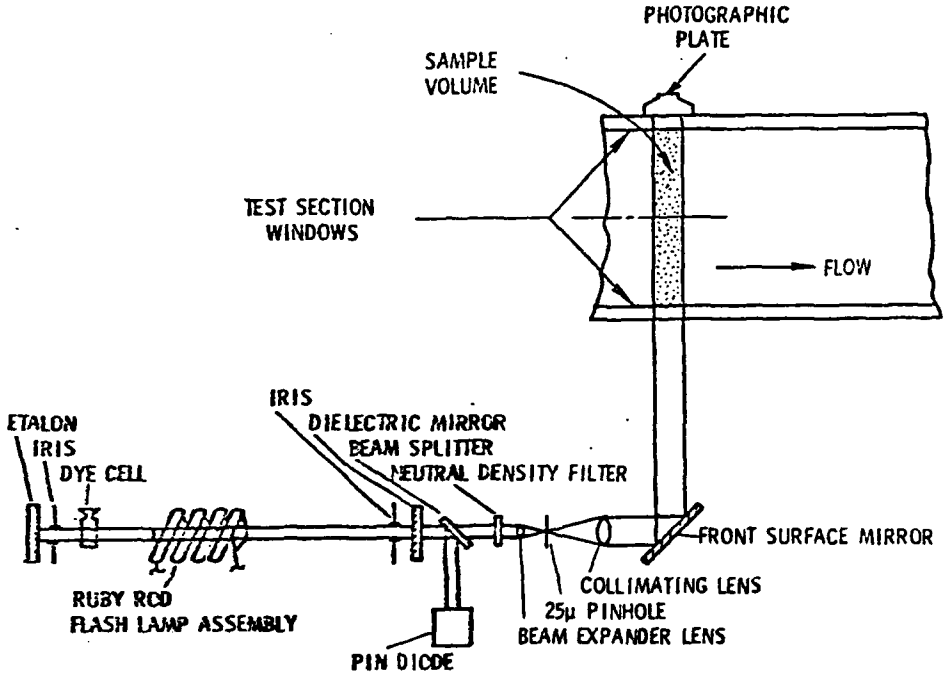

Figure 8. Schematic of Holographic System

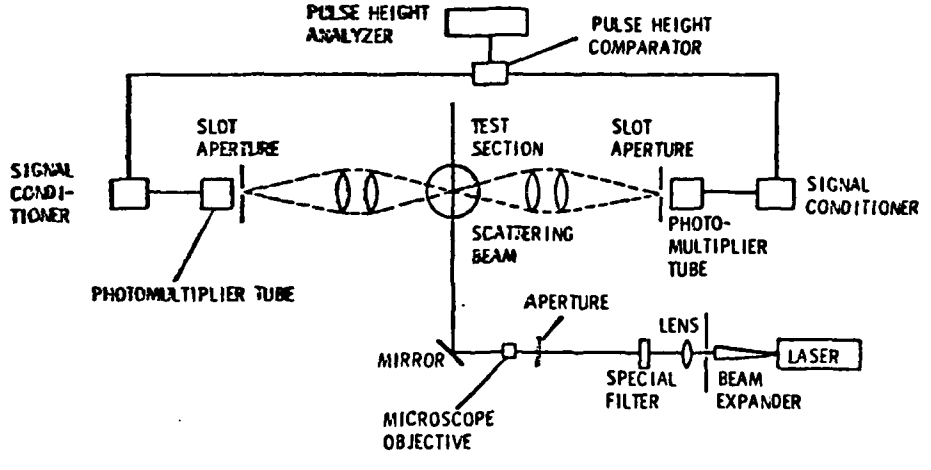

Figure 9. Schematic of the Dual-Detector Light Scattering System

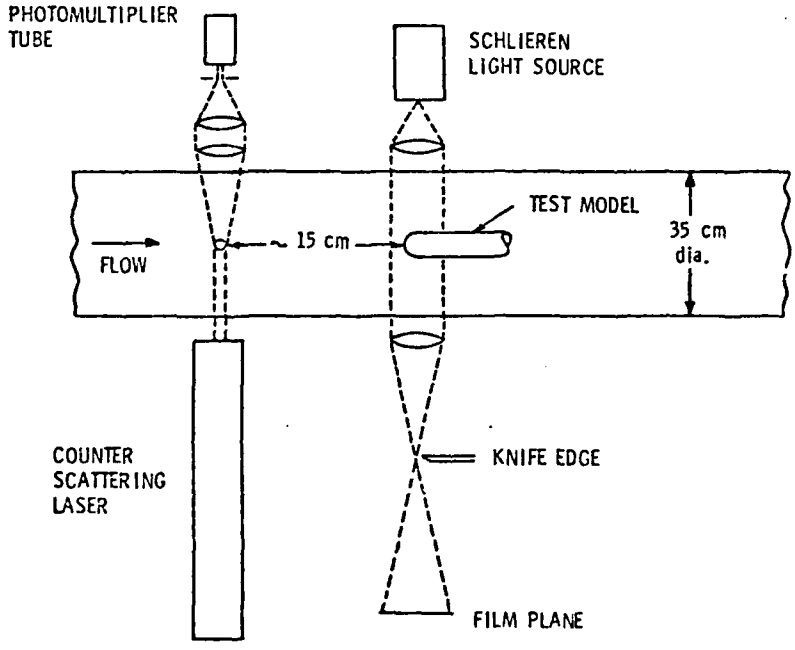

Figure 10. Schematic of the Schlieren Flow Visualization and Laser Light Scattering Systems

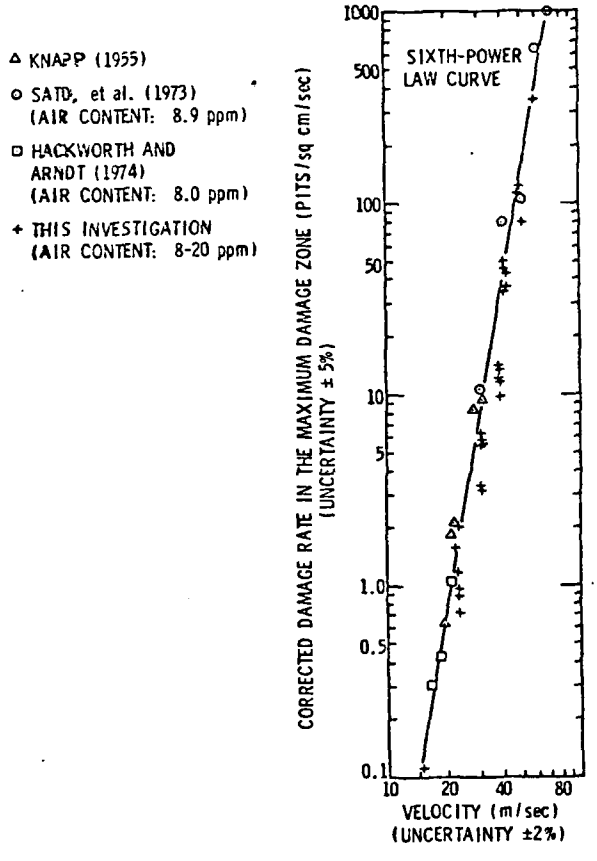

Figure 11. Damage Rate Versus Velocity From Various Investigations

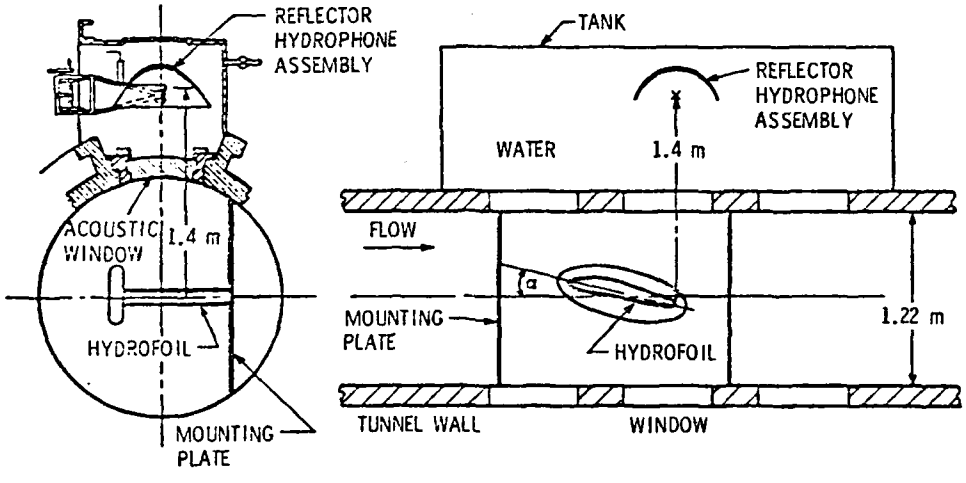

Figure 12. Acoustic Tank and Reflector Hydrophone Arrangement

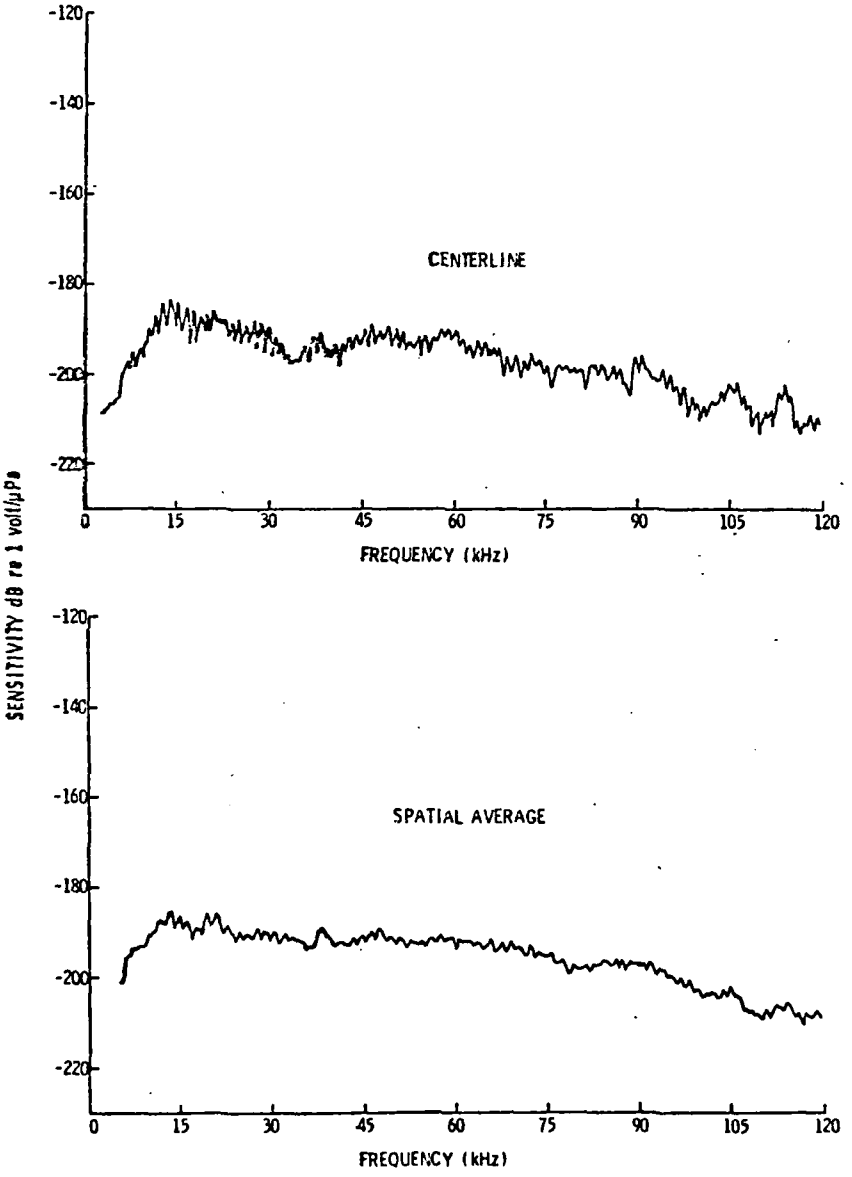

Figure 13. Typical Sensitivity Curves for Reflector Hydrophone (5-120 kHz) With Projector on Centerline and Spatially-Averaged for Several Projector Locations off Centerline

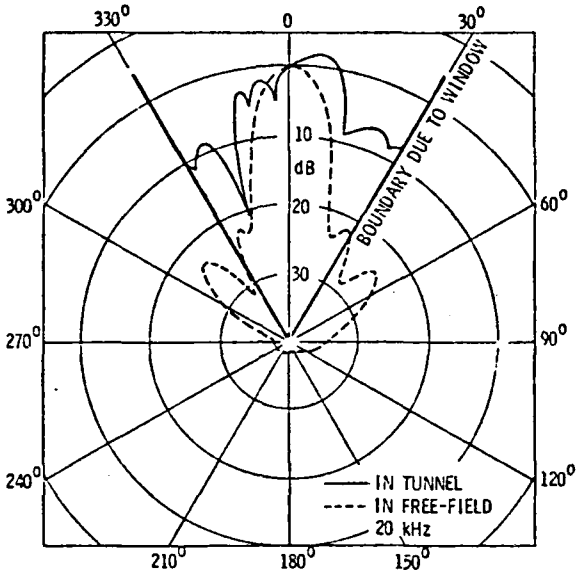

Figure 14. Reflector Hydrophone Directivity @ 20 kHz

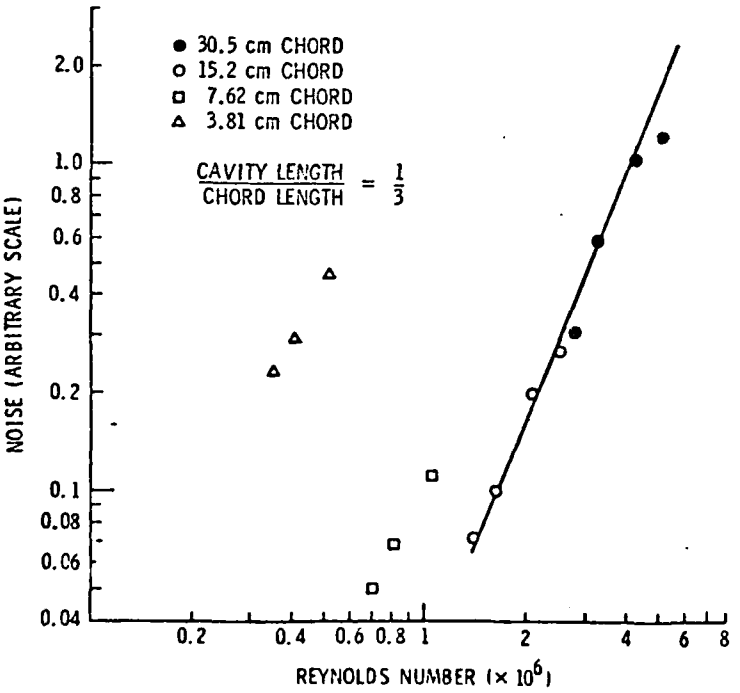

Figure 15. RMS Noise Level of Leading Edge Sheet Cavitation Versus Reynolds Number

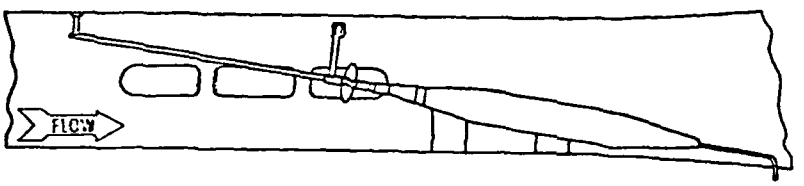

Figure 16. Installation of Ship Propeller in an Inclined Flow in GTWT

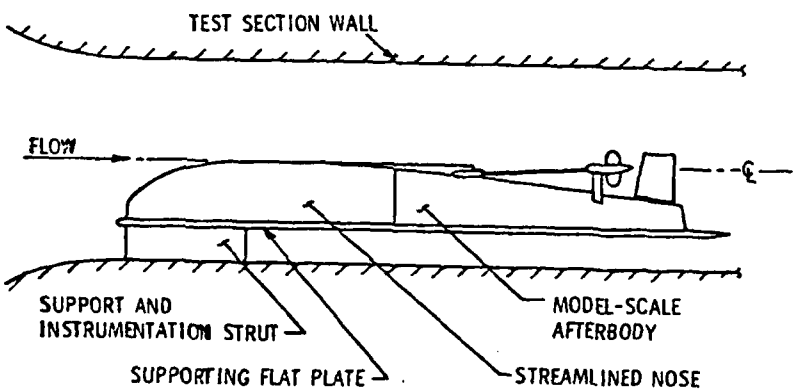

Figure 17. Installation of a Ship Model Hull and Propeller in GTWT

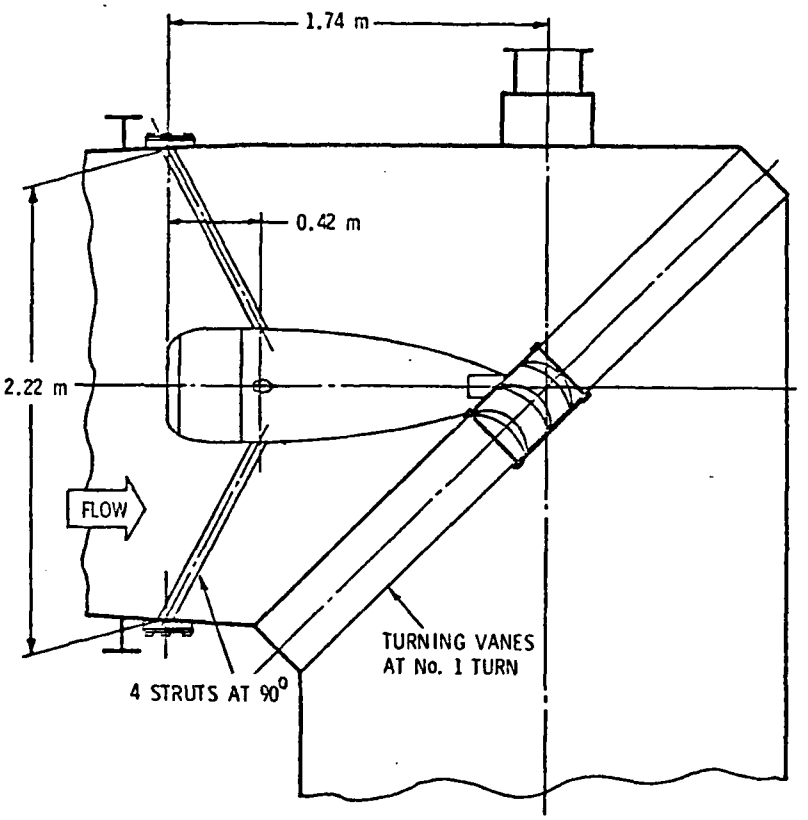

Figure 18. GTWT Downstream Array

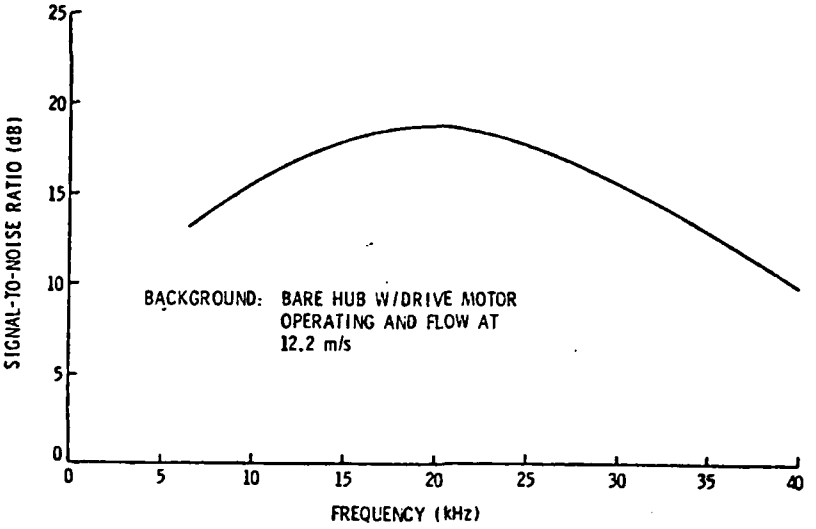

Figure 19. Typical Signal-to-Noise Ratio Measured With Non-Cavitating Propeller in GTWT

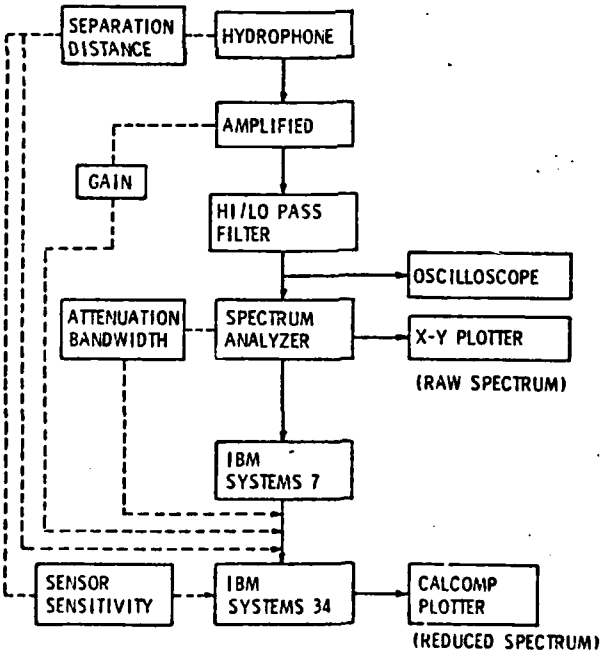

Figure 20. Block Diagram of Noise Data Reduction System

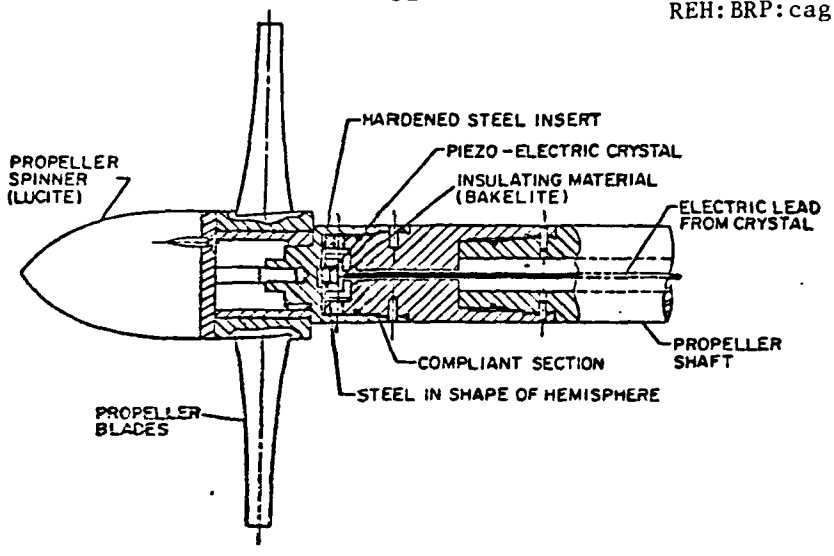

Figure 21. Dynamic Shaft Thrust Dynamometer

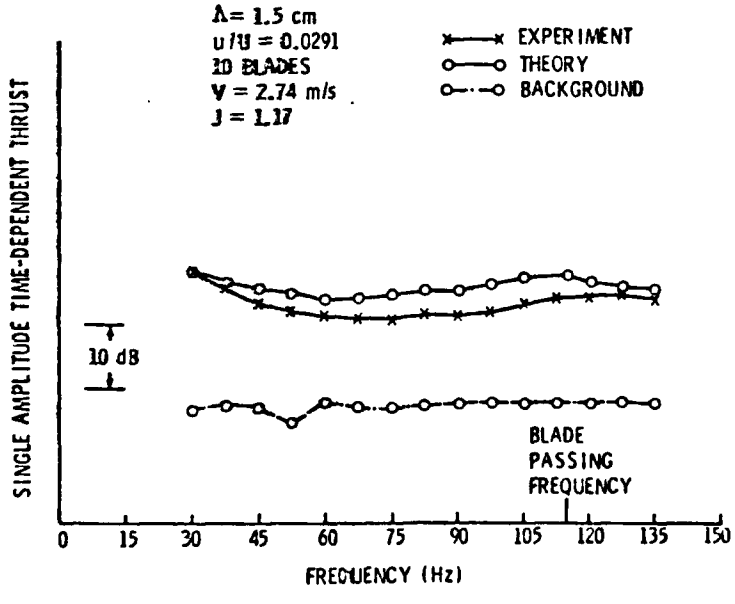

Figure 22. Turbulence Generated Dynamic Shaft Thrust

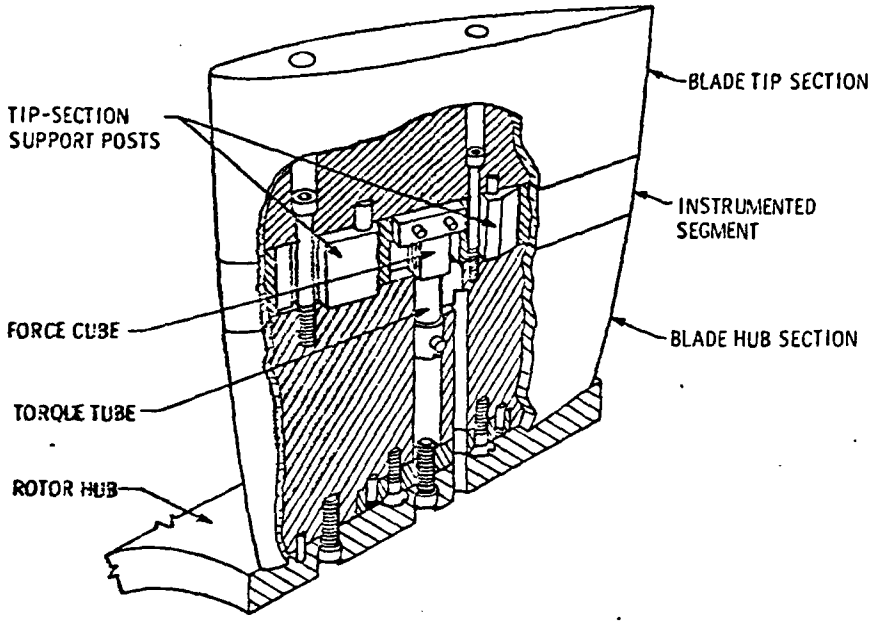

Figure 23. Dynamic Lift and Moment Dynamometer for a Rotating Blade

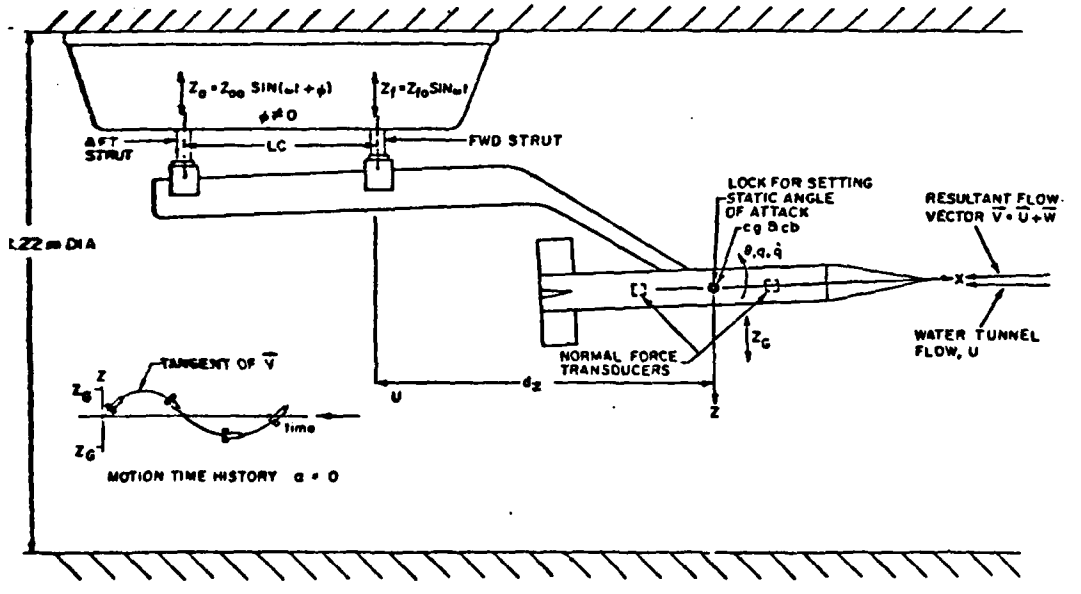

Figure 24. GTWT Planar Motion Mechanism

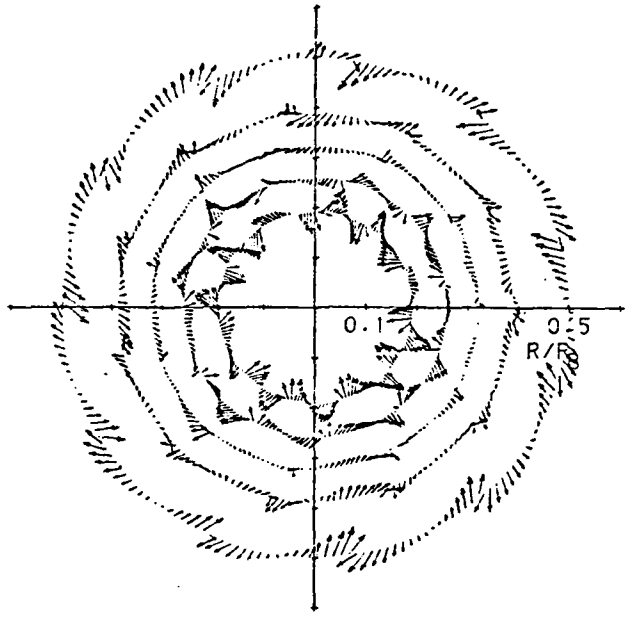

Figure 25. Radial and Tangential Velocity Vectors Measured Behind a Set of Stationary Fins

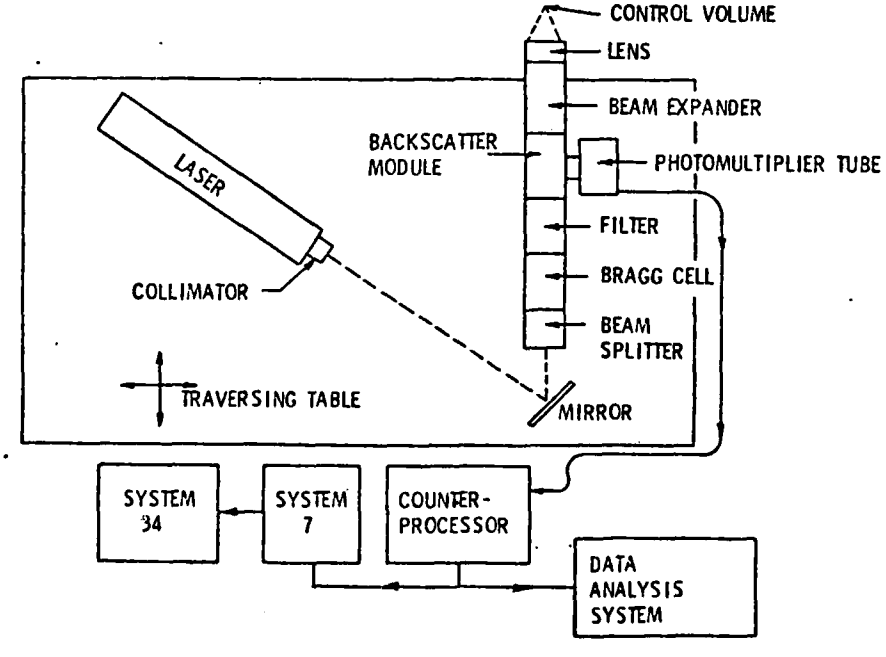

Figure 26. Laser Doppler Velocimeter for Measuring Velocities Relative to a Rotating Propeller

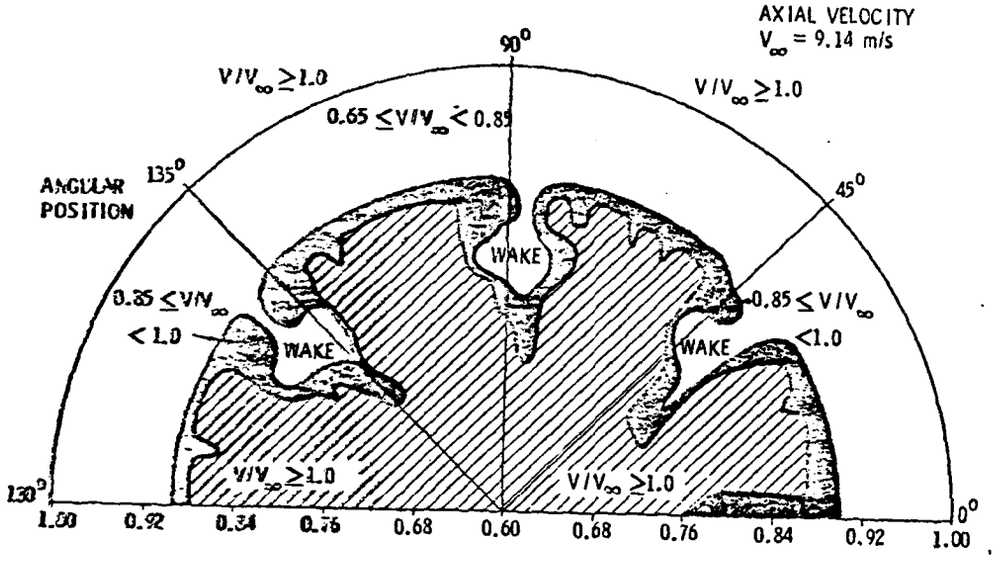

Figure 27. Axial Velocity Behind a Rotating Propeller; Relative to the Propeller

APPENDIX: FACILITY OPERATING CHARACTERISTICS

12 February 1982
REH:BRP:cag

APPLIED RESEARCH LABORATORY, FLUIDS ENGINEERING DEPARTMENT (USA)
THE PENNSYLVANIA STATE UNIVERSITY
P. O. BOX 30, STATE COLLEGE, PA 16801 (814) 865-1741

CAVITATION TUNNEL (Garfield Thomas) 1949

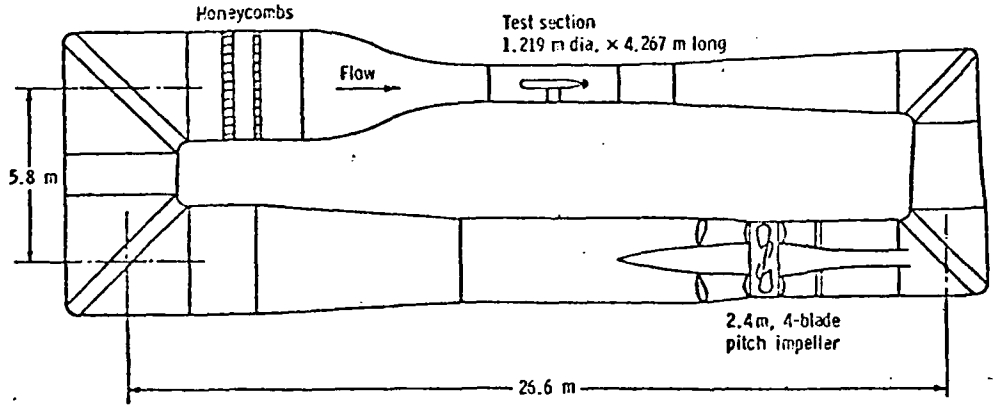

DESCRIPTION OF FACILITY:	Closed Circuit, Closed Jet
TYPE OF DRIVE SYSTEM:	4-Blade Adjustable Pitch Impeller
TOTAL MOTOR POWER:	2000 HP Variable Speed (1491 kw)
WORKING SECTION MAX. VELOCITY:	18.29 m/s
MAX. & MIN. ABS. PRESSURES:	413.7 to 20.7 kPa
CAVITATION NUMBER RANGE:	>0.1 dependent on velocity and/or J-range

INSTRUMENTATION: Propeller Dynamometers, 5-Hole Pitot Probes, Lasers, Pressure Sensors, Hydrophones, Planar Motion Mechanism, Force Balances

TYPE AND LOCATION OF TORQUE & THRUST DYNAMOMETERS: Model internally mounted, 140 HP limit. (104.40 kw)

PROPELLER OR MODEL SIZE RANGE: Model size from 76.2 mm to 635.0 mm dia.

TESTS PERFORMED: (1) Forces and pressure distributions on bodies of revolution, hydrofoils, propellers, etc., (2) Cavitation performance and noise measurements of propellers, foils, hydrodynamic shapes, etc., (3) Steady state and time-dependent force and torque measurements on powered models.

OTHER REMARKS: Tunnel turbulence level is 0.1 percent in test section. Air content can be controlled as low as 1 ppm per mole. Measurement can be made of hydrodynamic functions for stability and control of submerged vehicles. Directional hydrophone system for relative acoustic measurements.

PUBLISHED DESCRIPTION: ARL/PSU Report NORD 16597-56, Lehman, 1959

12 February 1982
REH:BRP:cag

APPLIED RESEARCH LABORATORY, FLUIDS ENGINEERING DEPARTMENT (USA)
THE PENNSYLVANIA STATE UNIVERSITY
P. O. BOX 30, STATE COLLEGE, PA 16801 (814) 865-1741

CAVITATION TUNNEL 1951

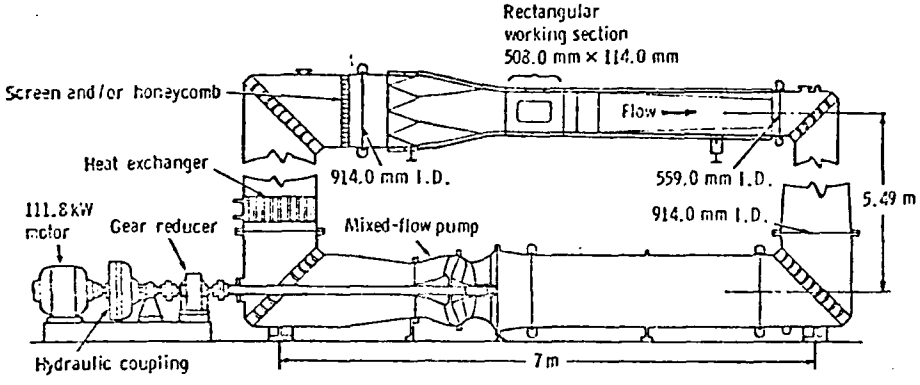

DESCRIPTION OF FACILITY:	Closed Circuit, Closed Jet
TEST SECTIONS:	1) Circular: 304.8 mm dia. x 762.0 mm long 2) Rectangular: 508.0 mm x 114.3 mm x 762.0 mm long
TYPE OF DRIVE SYSTEM:	Mixed Flow Peerless Pump
TOTAL MOTOR POWER:	150 HP (111.8 kw)
WORKING SECTION MAX. VELOCITY:	24.38 m/s
MAX. & MIN. ABS. PRESSURES:	413.7 to 20.7 kPa
CAVITATION NUMBER RANGE:	>0.1 dependent on velocity

INSTRUMENTATION: Lasers, pressure sensors, hydrophones

MODEL SIZE RANGE: 50.8 mm max. dia.

TESTS PERFORMED: Steady and time dependent force and pressure measurements on unpowered models. Noise measurements on cavitating models. Three-dimensional flow problems—circular section. Two-dimensional flow problems—rectangular section. Axial-flow pump tests.

OTHER REMARKS: Independent gas control of air content. Water filtration with 25-micrometer filters. Intermittent operation with drag-reducing additive injection. Partial neutralization of additive downstream of test section.

PUBLISHED DESCRIPTION: ARL/PSU Report NORD 16597-56, Lehman, 1959

12 February 1982
REH:BRP:cag

APPLIED RESEARCH LABORATORY, FLUIDS ENGINEERING DEPARTMENT (USA)
THE PENNSYLVANIA STATE UNIVERSITY
P. O. BOX 30, STATE COLLEGE, PA 16801 (814) 865-1741

CAVITATION TUNNEL 1962

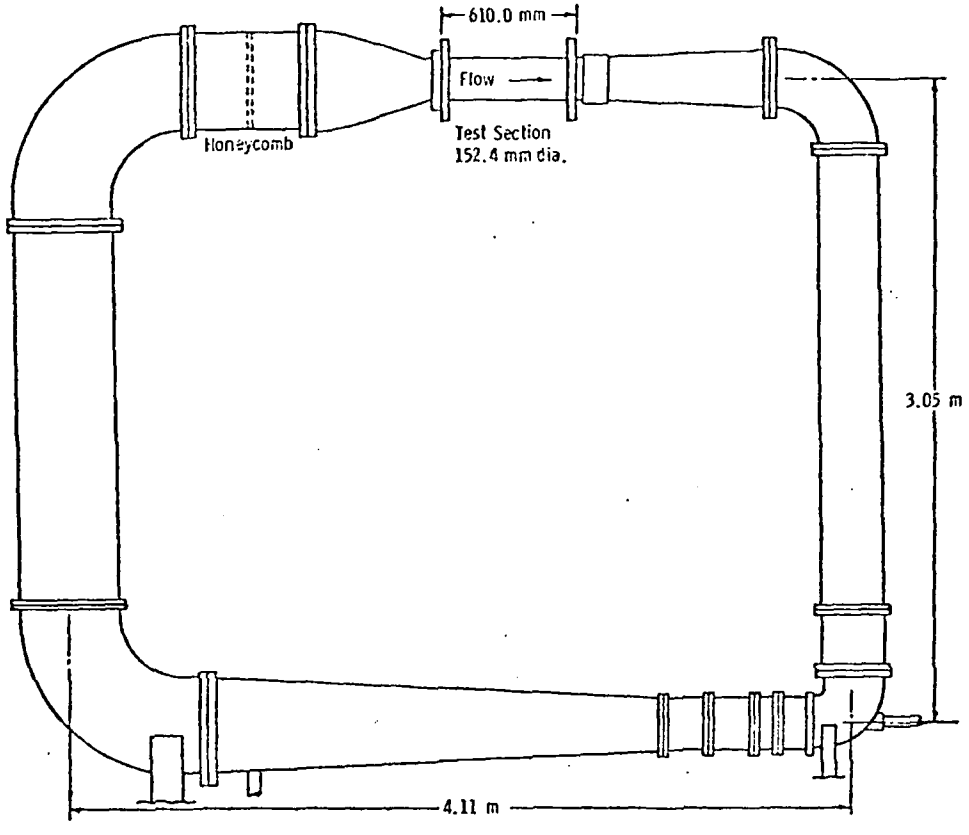

DESCRIPTION OF FACILITY:	Closed Circuit, Closed Jet
TYPE OF DRIVE SYSTEM:	Axial-Flow Pump
TOTAL MOTOR POWER:	25 HP (18.64 kw)
WORKING SECTION MAX. VELOCITY:	21.34 m/s
MAX. & MIN. ABS. PRESSURES:	861.9 to 20.7 kPa
CAVITATION NUMBER RANGE:	>0.1 dependent on velocity and pressure

INSTRUMENTATION: Pressure Transducers

TEMPERATURE: Ambient

TESTS PERFORMED: Effect of polymers on axial-flow pumps. Surface roughness effects on cavitation.

OTHER REMARKS: Air content control by vacuum pump. Filtration of solid particles and non-Newtonian additives by activated charcoal.

PUBLISHED DESCRIPTION: PSU M.S. Thesis, Kaku, 1962

12 February 1982
REH:BRP:cag

APPLIED RESEARCH LABORATORY, FLUIDS ENGINEERING DEPARTMENT (USA)
THE PENNSYLVANIA STATE UNIVERSITY
P. O. BOX 30, STATE COLLEGE, PA 16801 (814) 865-1741

ULTRA-HIGH SPEED CAVITATION TUNNEL 1960

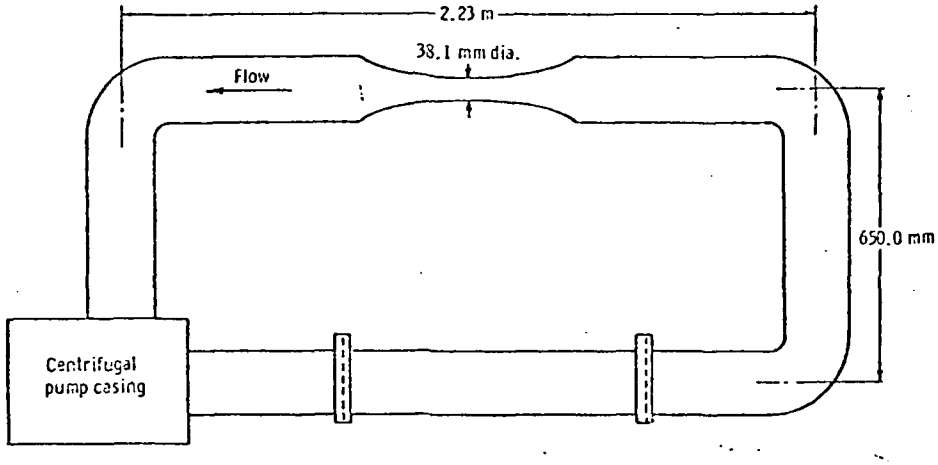

DESCRIPTION OF FACILITY:	Closed Circuit, Closed Jet
TYPE OF DRIVE SYSTEM:	Centrifugal Variable Speed Drive
TOTAL MOTOR POWER:	75 HP (55.9 kw)
WORKING SECTION MAX. VELOCITY:	83.8 m/s
MAX. & MIN. ABS. PRESSURES:	8274.0 to 41.4 kPa
CAVITATION NUMBER RANGE:	>0.01 dependent on pressure and velocity

INSTRUMENTATION: Pressure and temperature sensors

TEMPERATURE RANGE: 16°C to +176°C

MODEL SIZE RANGE: 12.7 mm max. dia.

TEST MEDIUM: Water, Freon 113, Alcohol

TESTS PERFORMED: Incipient and desinent cavitation studies. Developed cavitation studies. Cavitation damage.

OTHER REMARKS: Stainless steel tunnel. Bronze pump. Three filter banks for removal of water, acids, solid particles (10 micrometers).

PUBLISHED DESCRIPTION: ARL/PSU TM 75-188, Weir, Billet & Holl, 1975

12 February 1982
REH:BRP:cag

APPLIED RESEARCH LABORATORY, FLUIDS ENGINEERING DEPARTMENT (USA)
THE PENNSLYVANIA STATE UNIVERSITY
P. O. BOX 30, STATE COLLEGE, PA 16801 (814) 865-1741

AXIAL FLOW RESEARCH FAN 1971

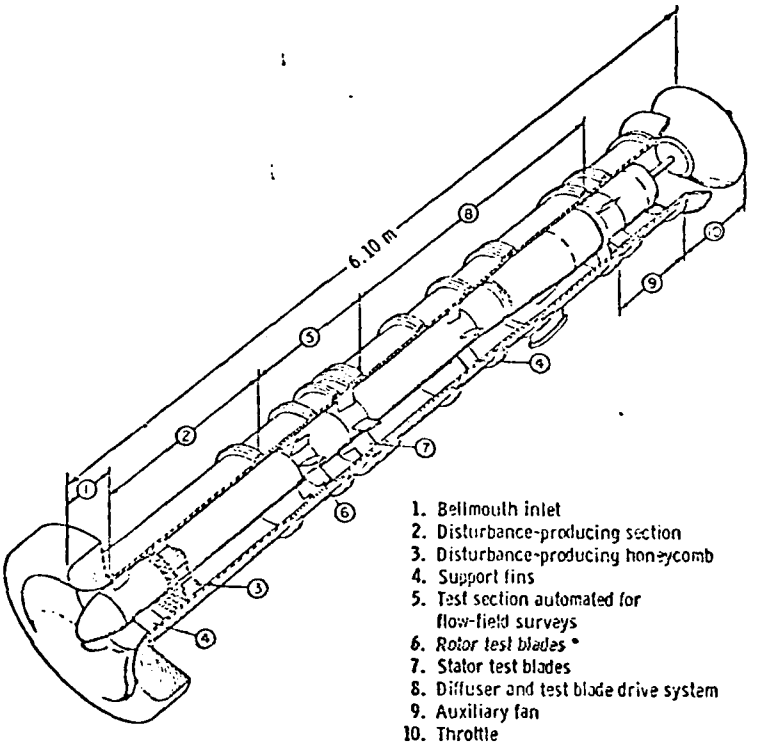

*540.0 mm O.D., 241.0 mm hub dia., 150.0 mm blade chord

DESCRIPTION OF FACILITY:	Open Circuit
TYPE OF DRIVE SYSTEM:	Single Axial Flow Stage
TOTAL MOTOR POWER:	20 HP (14.9 kw)
WORKING SECTION MAX. VELOCITY:	34.14 m/s through-flow velocity
MAX. RELATIVE VELOCITY:	91.44 m/s

INSTRUMENTATION: Variable geometry test stage. Instrumented blade for measuring unsteady lift and pitching moment. Rotating outer casing for flow surveys. Distortion screens to produce reduced frequencies between 0.25 and 5.0.

TESTS PERFORMED: Measurements in a distorted inflow of the unsteady lift, moment, surface pressures, instantaneous total pressure and time mean velocities and pressures, as a function of stage geometry and reduced frequency.

OTHER REMARKS: Facility was specifically built for research in the generating mechanism of turbomachinery noise and vibration, a problem which is of significance in many areas of engineering, including that of environmental pollution.

PUBLISHED DESCRIPTION: ARL/PSU TM 72-109, Bruce, 1972

DISTRIBUTION LIST FOR UNCLASSIFIED ARL TM No. 82-66 by R. E. Henderson and B. R. Parkin, dated 12 February 1982.

Commander
Naval Sea Systems Command
Department of the Navy
Washington, DC 20362
Attn: Library
Code NSEA-09G32
(Copy Nos. 1 and 2)

Naval Sea Systems Command
Attn: R. Keane
Code NSEA-3213
(Copy No. 3)

Naval Sea Systems Command
Attn: C. Mussen
Code PMS-3962
(Copy No. 4)

Naval Sea Systems Command
Attn: F. E. Eissing
Code NSEA-05H
(Copy No. 5)

Naval Sea Systems Command
Attn: S. M. Blazek
Code NSEA-05HB
(Copy No. 6)

Naval Sea Systems Command
Attn: A. R. Paladino
Code NSEA-05H1
(Copy No. 7)

Naval Sea Systems Command
Attn: F. B. Peterson
Code NSEA-052P
(Copy No. 8)

Naval Sea Systems Command
Attn: F. J. Welling
Code NSEA-521
(Copy No. 9)

Naval Sea Systems Command
Attn: R. Taddeo
Code NSEA-5212
(Copy No. 10)

Naval Sea Systems Command
Attn: E. G Liszka
Code NSEA-63R1
(Copy No. 11)

Naval Sea Systems Command
Attn: F. J. Romano
Code NSEA-63R3
(Copy No. 12)

Naval Sea Systems Command
Attn: T. E. Peirce
Code NSEA-63R31
(Copy No. 13)

Naval Sea Systems Command
Attn: R. Cauley
Code NSEA-052B
(Copy No. 14)

Naval Sea Systems Command
Attn: R. A. Johnson
Code NSEA-03D35
(Copy No. 15)

Naval Sea Systems Command
Attn: C. D. Smith
Code NSEA-06R
(Copy No. 16)

Naval Sea Systems Command
Attn: E. M. Peebles
Code NSEA-92
(Copy No. 17)

Naval Sea Systems Command
Attn: D. M. Jackson
Code NSEA-06B
(Copy No. 18)

Naval Sea Systems Command
Attn: T. M. Hopkins
Code NSEA-05
(Copy No. 19)

Naval Sea Systems Command
Attn: M. V. Ricketts
Code NSEA-03
(Copy No. 20)

Commanding Officer
Naval Underwater Systems Center
Newport, RI 02840
Attn: D. Goodrich
Code 3634
(Copy No. 21)

DISTRIBUTION LIST FOR UNCLASSIFIED ARL TM No. 82-66 by R. E. Henderson and B. R. Parkin, dated 12 February 1982.

Naval Underwater Systems Center
Attn: B. J. Myers
Code 36311
(Copy No. 22)

Naval Underwater Systems Center
Attn: R. H. Nadolink
Code 3634
(Copy No. 23)

Naval Underwater Systems Center
Attn: R. Kittredge
Code 36301
(Copy No. 24)

Naval Underwater Systems Center
Attn: Library
Code 54
(Copy No. 25)

Officer-in-Charge
David W. Taylor Naval Ship R&D Center
Department of the Navy
Annapolis Laboratory
Annapolis, MD 21402
Attn: E. R. Quandt
Code 272
(Copy No. 26)

David W. Taylor Naval Ship R&D Center
Attn: J. V. Pierpoint
Code 2741
(Copy No. 27)

David W. Taylor Naval Ship R&D Center
Attn: J. Henry
Code 2741
(Copy No. 28)

David W. Taylor Naval Ship R&D Center
Attn: Y. F. Wang
Code 2740
(Copy No. 29)

Commander
David W. Taylor Naval Ship R&D Center
Department of the Navy
Bethesda, MD 20084
Attn: W. B. Morgan
Code 15
(Copy No. 30)

David W. Taylor Naval Ship R&D Center
Attn: Library
Code 1505
(Copy No. 31)

David W. Taylor Naval Ship R&D Center
Attn: W. G. Day
Code 1521
(Copy No. 32)

David W. Taylor Naval Ship R&D Center
Attn: A. C. Lin
Code 1521
(Copy No. 33)

David W. Taylor Naval Ship R&D Center
Attn: R. A. Cumming
Code 1540
(Copy No. 34)

David W. Taylor Naval Ship R&D Center
Attn: J. H. McCarthy
Code 154
(Copy No. 35)

David W. Taylor Naval Ship R&D Center
Attn: T. E. Brockett
Code 1544
(Copy No. 36)

David W. Taylor Naval Ship R&D Center
Attn: M. M. Sevik
Code 19
(Copy No. 37)

David W. Taylor Naval Ship R&D Center
Attn: W. K. Blake
Code 1905
(Copy No. 38)

David W. Taylor Naval Ship R&D Center
Attn: F. S. Archibald
Code 1942
(Copy No. 39)

Commander
Naval Surface Weapons Center
Silver Spring, MD 20910
Attn: Library
(Copy No. 40)

DISTRIBUTION LIST FOR UNCLASSIFIED ARL TM No. 82-66 by R. E. Henderson and B. R. Parkin, dated 12 February 1982.

Office of Naval Research
Department of the Navy
800 N. Quincy Street
Arlington, CA 22217
Attn: A. H. Gilmore
(Copy No. 41)

Office of Naval Research
Attn: Adm. Kollmorgen
(Copy No. 42)

Office of Naval Research
Attn: R. Whitehead
(Copy No. 43)

Office of Naval Research
Attn: C. Lee
(Copy No. 44)

Commanding Officer
Naval Ocean Systems Center
San Diego, CA 92152
Attn: Library
(Copy No. 45)

Naval Ocean Systems Center
Attn: M. M. Reischmann
(Copy No. 46)

Naval Ocean Systems Center
Attn: D. Nelson
(Copy No. 47)

Naval Ocean Systems Center
Attn: J. Green
(Copy No. 48)

Defense Technical Information Center
5010 Duke Street
Cameron Station
Alexandria, VA 22314
(Copy Nos. 49 to 54)

Commanding Officer
Naval Underwater Systems Center
Newport, RI 02840
Attn: P. Tabor
(Copy No. 55)

Naval Underwater Systems Center
Attn: P. LaBrecque
(Copy No. 56)

Dr. G. F. Wislicenus
351 Golf Court (Oakmont)
Santa Rosa, CA 95405
(Copy No. 57)

J. M. Robertson
125 Talbot Laboratory
University of Illinois
Urbana, IL 61801
(Copy No. 58)

The Pennsylvania State University
Applied Research Laboratory
Post Office Box 30
State College, PA 16801
Attn: M. L. Billet
(Copy No. 59)

Applied Research Laboratory
Attn: W. S. Gearhart
(Copy No. 60)

Applied Research Laboratory
Attn: G. B. Gurney
(Copy No. 61)

Applied Research Laboratory
Attn: W. R. Hall
(Copy No. 62)

Applied Research Laboratory
Attn: J. W. Holl
(Copy No. 63)

Applied Research Laboratory
Attn: G. C. Lauchle
(Copy No. 64)

Applied Research Laboratory
Attn: F. E. Smith
(Copy No. 65)

Applied Research Laboratory
Attn: D. E. Thompson
(Copy No. 66)

Applied Research Laboratory
Attn: A. L. Treaster
(Copy No. 67)

Applied Research Laboratory
Attn: R. E. Henderson
(Copy No. 68)

DISTRIBUTION LIST FOR UNCLASSIFIED ARL TM No. 82-66 by R. E. Henderson and B. R. Parkin, dated 12 February 1982.

Applied Research Laboratory
Attn: B. R. Parkin
(Copy No. 69)

Applied Research Laboratory
Attn: GTWT Files
(Copy No. 70)

R. Leitner
DARPA (TTO)
1400 Wilson Blvd.
Arlington, VA 22209
(Copy No. 71)

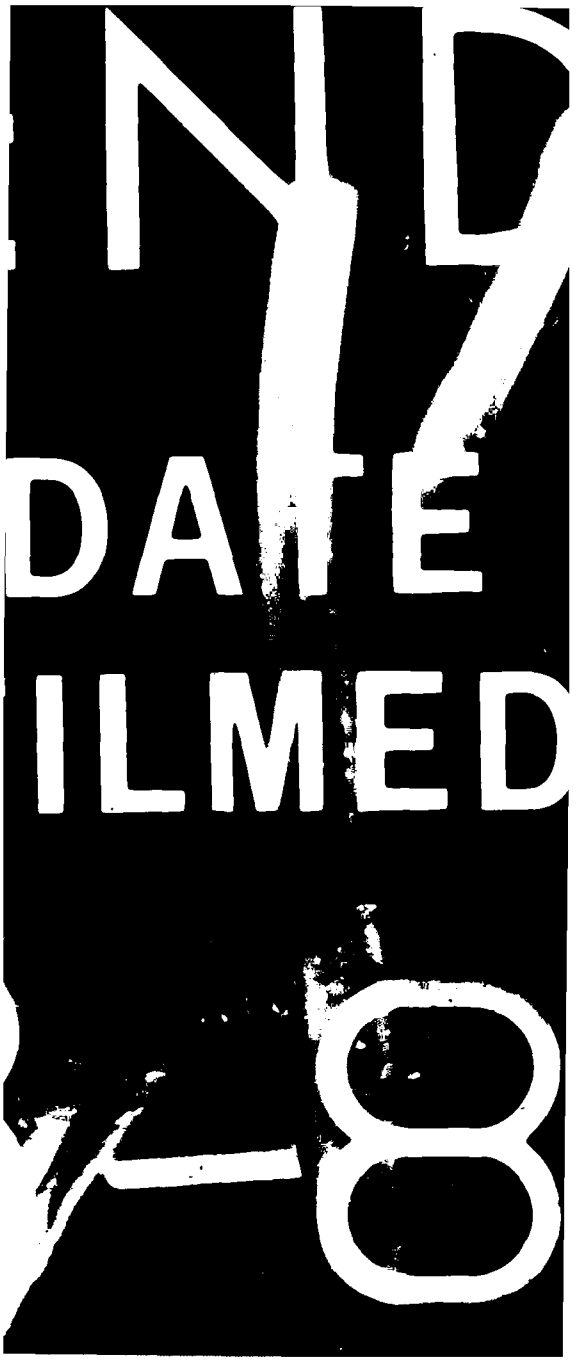
DATE
ILMED
7-8

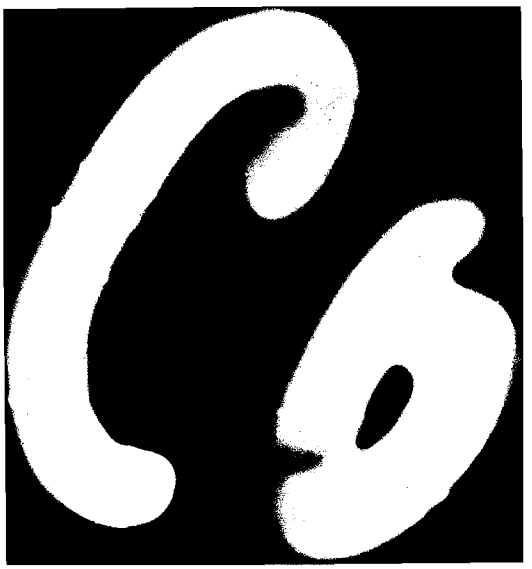

AD-A116 292 PENNSYLVANIA STATE UNIV UNIVERSITY PARK APPLIED RESE--ETC F/6 14/2
HYDRODYNAMIC TEST FACILITIES AT ARL/PSU.(U)
FEB 82 R E HENDERSON, B R PARKIN N00024-79-C-6043
UNCLASSIFIED ARL/PSU/TM-82-66 NL

END
DATE FILMED
9-82
DTIC


DA
I 6

SUPPLEMENTARY

INFORMATION

THE PENNSYLVANIA STATE UNIVERSITY
INTERCOLLEGE RESEARCH PROGRAMS AND FACILITIES
APPLIED RESEARCH LABORATORY

ADDRESS REPLY TO:
APPLIED RESEARCH LABORATORY
P. O. BOX 30
STATE COLLEGE, PENNSYLVANIA 16801

August 10, 1982

TO: Distribution List

SUBJECT: Corrected Page for ARL Technical Memorandum

A typographical error has been found on the first line of Page 8 of ARL TM 82-66, "Hydrodynamic Test Facilities at ARL/PSU," by R. E. Henderson and B. R. Parkin, 12 February 1982.

Please replace Page 7-8 in your copy(ies) with the attached.

Very truly yours,

Blaine R. Parkin

Blaine R. Parkin
Director
Garfield Thomas Water Tunnel

BRP:mac

was concluded from these experiments that the light scattering technique was not able to discriminate between solid particles and air bubbles in the flow.

As a result of these findings, recent studies at ARL/PSU have concentrated on the development of a dual-detector technique which, with the use of Mie-scattering theory, can give information about the shape of the particle. This permits the light scattering technique to discriminate between microbubbles and particulates, Figure 9. The results to date indicate that this modified Keller system offers the potential of screening particulates from the microbubble counts [10]. The main task remaining before this approach can be called successful is to conduct a detail error analysis in order to resolve the system inaccuracy introduced by the data reduction algorithm. Because the light scattering technique offers the chance of getting nearly real-time nuclei distribution data while a cavitation test is in progress, this improvement of the Keller system is worth pursuing.

Assuming that valid nuclei size distributions can be obtained while a cavitation experiment is underway, the question of how such distributions influence the development of cavitation on a body must be studied. Such a study can be conducted if the cavitation events can be related to such flow features as the boundary layer thickness or whether or not the flow is separated. Schlieren flow visualization is an effective way to show the relationship of cavitation inception and its type to the state of the boundary layer [11]. Measurements of this type have been performed in the ARL/PSU 0.305 m tunnel using light scattering and schlieren systems simultaneously as illustrated in Figure 10 [12].

Of course holographic photography can be used for flow visualization with excellent results in both cavitating and non-cavitating flows.

4.2 Cavitation Damage

In the introductory remarks of this section it was noted that one use of the NASA tunnel and its very high velocity, has been to study the process of cavitation damage [13]. Recent studies at ARL/PSU have confirmed the sixth-power of the free-stream velocity scaling relation reported by previous investigators. In these studies it was possible to obtain nearly a four-fold increase in velocity, from about 15 m/s to 60 m/s. A fact not previously reported is that the pitting rate in the incubation zone is sensitive to, and inversely proportional to, the dissolved air content. Therefore it was possible to correct all of the data to a standard air content of 8.9 ppm so that data for all investigations over a 10,000 to 1 range in damage rates could be brought into remarkable agreement, Figure 11. It is important to stress that this investi-

gation involved the study of pitting on a body without the occurrence of weight loss. With this restriction it was found that damage in the form of individual pits had a one-to-one correspondence with the cavitation bubble collapse energy, and the change in this energy with free-stream velocity could be inferred.

5.0 ACOUSTIC TESTS

The GTWT was designed to provide the capability to conduct research on torpedo propellers operated in a specified vehicle/control fin wake [1]. With the wake flow produced by the installation of the actual vehicle or a scaled model, the measurement of the forces on the vehicle and its propeller and the occurrence of cavitation on the propeller were the primary performance characteristics studied. While the inception of cavitation was detected acoustically, as well as visually, the GTWT was not used to conduct detailed acoustic tests during its first 20 years of operation. Fortunately, the design of the GTWT was directed towards quiet and vibration free operation. The success in achieving these goals has permitted the development of a capability to conduct tests of both cavitating and non-cavitating propeller noise.

5.1 Cavitation Noise

The GTWT was designed so that one side of its test section could be fitted with an acoustic tank in which a traversing reflector hydrophone could be mounted, Figure 12. With the hydrophone focused on the centerline of the test section, it measures the noise radiated from a model located opposite the 27 cm x 60 cm plexiglass windows.

The receiver is a Celesco LC-10 hydrophone located at the focus of the ellipsoidal reflector. This hydrophone is calibrated by placing an omni-directional sound projector with a known response in the test section and driving it over a frequency range of 1-120 kHz. The calibration is conducted with the sound projector located on the test section centerline and at a constant distance off-centerline in each of four or more circumferential positions, Figure 13. This latter approach permits an average sensitivity to be determined diminishes the influence of spurious acoustic modes that are observed when the projector is on the centerline. It is also more representative of the noise radiated by a propeller since cavitation will normally appear first near the tip of the blades.

The influence of the test section on the directivity of the reflector hydrophone is shown by Figure 14. In this figure the directivity measured at 20 kHz in the test section is compared with the same measurement conducted in the free field [14]. It is obvious that this arrangement is acceptable if the hydrophone is positioned in the center of the window, but is restricted by the metal webs between the windows. To overcome this restriction an